Article

Cell Reports

The Mitochondrial Apoptotic Effectors BAX/BAK Activate Caspase-3 and -7 to Trigger NLRP3 Inflammasome and Caspase-8 Driven IL-1β Activation

Graphical Abstract

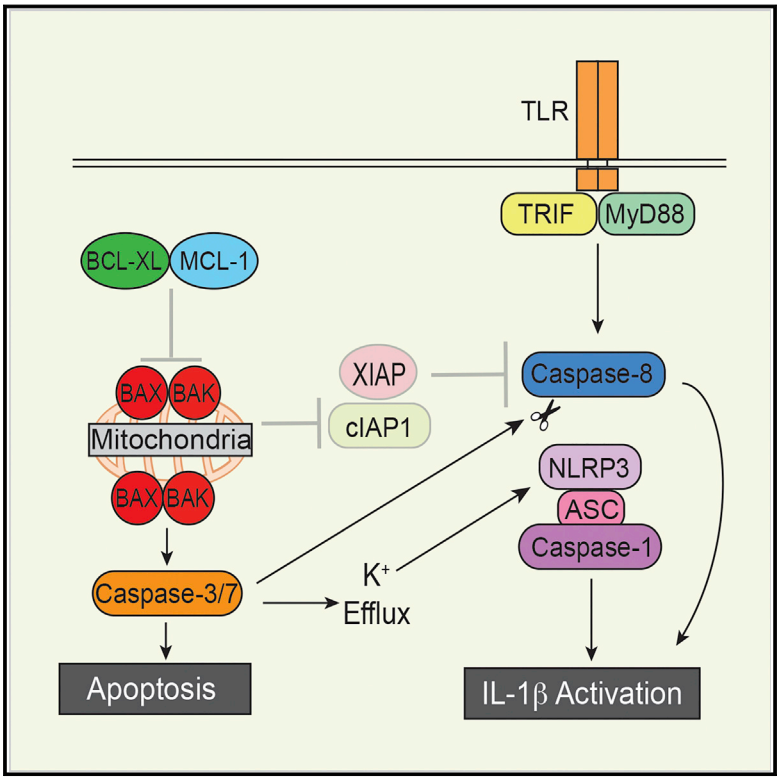

Authors

James E. Vince, Dominic De Nardo, Wenqing Gao, ..., Benjamin T. Kile, Feng Shao, Kate E. Lawlor

Correspondence

vince@wehi.edu.au (J.E.V.), kate.lawlor@hudson.org.au (K.E.L.)

In Brief

BAX/BAK-mediated apoptosis is considered immunologically silent. Vince et al. show that in macrophages, MCL-1 and BCL-XL restrain BAX/BAK-induced pro-inflammatory IL-1β activation. IAP degradation and activation of caspase-3 and -7 downstream of BAX/BAK triggers caspase-8-mediated cleavage and activation of IL-1β and cause potassium ion efflux to trigger NLRP3 inflammasome formation.

Highlights

- MCL-1 and BCL-XL prevent BAX/BAK-induced IL-1β activation and death in macrophages
- BAX/BAK-induced IL-1β requires the downstream effector caspases, caspase-3 and -7
- Caspase-3/-7 cause potassium efflux to activate the NLRP3 inflammasome and IL-1β
- BAX/BAK-induced caspase-3/-7 and IAP loss also trigger caspase-8 to cleave IL-1β

Vince et al., 2018, Cell Reports *25*, 2339–2353
November 27, 2018
https://doi.org/10.1016/j.celrep.2018.10.103

CellPress

Cell Reports
Article

The Mitochondrial Apoptotic Effectors BAX/BAK Activate Caspase-3 and -7 to Trigger NLRP3 Inflammasome and Caspase-8 Driven IL-1β Activation

James E. Vince,[1,2,*] Dominic De Nardo,[1,2,8] Wenqing Gao,[3,8] Angelina J. Vince,[1] Cathrine Hall,[1] Kate McArthur,[1,2,4] Daniel Simpson,[1,2] Swarna Vijayaraj,[1,2] Lisa M. Lindqvist,[1,2] Philippe Bouillet,[1,2] Mark A. Rizzacasa,[5] Si Ming Man,[6] John Silke,[1,2] Seth L. Masters,[1,2] Guillaume Lessene,[1,2] David C.S. Huang,[1,2] Daniel H.D. Gray,[1,2] Benjamin T. Kile,[1,2,4] Feng Shao,[3] and Kate E. Lawlor[1,2,7,9,*]

[1]The Walter and Eliza Hall Institute of Medical Research, Parkville, VIC 3052, Australia
[2]Department of Medical Biology, University of Melbourne, Parkville, VIC 3010, Australia
[3]National Institute of Biological Sciences, Beijing 102206, China
[4]Anatomy and Developmental Biology, Monash Biomedicine Discovery Institute, Monash University, Clayton, VIC 3800, Australia
[5]School of Chemistry, The Bio 21 Institute, The University of Melbourne, Melbourne, VIC 3010, Australia
[6]Department of Immunology and Infectious Disease, The John Curtin School of Medical Research, Australian National University, Canberra 2601, Australia
[7]Present address: Centre for Innate Immunity and Infectious Diseases, Hudson Institute of Medical Research, Department of Molecular and Translational Science, Monash University, Clayton, VIC 3168, Australia
[8]These authors contributed equally
[9]Lead Contact
*Correspondence: vince@wehi.edu.au (J.E.V.), kate.lawlor@hudson.org.au (K.E.L.)
https://doi.org/10.1016/j.celrep.2018.10.103

SUMMARY

Intrinsic apoptosis resulting from BAX/BAK-mediated mitochondrial membrane damage is regarded as immunologically silent. We show here that in macrophages, BAX/BAK activation results in inhibitor of apoptosis (IAP) protein degradation to promote caspase-8-mediated activation of IL-1β. Furthermore, BAX/BAK signaling induces a parallel pathway to NLRP3 inflammasome-mediated caspase-1-dependent IL-1β maturation that requires potassium efflux. Remarkably, following BAX/BAK activation, the apoptotic executioner caspases, caspase-3 and -7, act upstream of both caspase-8 and NLRP3-induced IL-1β maturation and secretion. Conversely, the pyroptotic cell death effectors gasdermin D and gasdermin E are not essential for BAX/BAK-induced IL-1β release. These findings highlight that innate immune cells undergoing BAX/BAK-mediated apoptosis have the capacity to generate pro-inflammatory signals and provide an explanation as to why IL-1β activation is often associated with cellular stress, such as during chemotherapy.

INTRODUCTION

Mitochondrial or "intrinsic" apoptosis is an evolutionarily conserved, BCL-2 family-regulated process that promotes the death and phagocytic clearance of stressed, damaged, or infected cells. Triggered by a diverse range of cellular stressors, such as growth factor withdrawal, infection, and anti-cancer chemotherapeutics, intrinsic apoptosis ensues when activated BAX and/or BAK oligomers insert into and permeabilize the mitochondrial outer membrane, releasing cytochrome *c* into the cytosol (Strasser and Vaux, 2018). Subsequently, cytosolic cytochrome *c* nucleates formation of the cytochrome *c*/APAF-1/caspase-9 apoptosome. Active caspase-9 in turn engages executioner caspases, such as caspase-3 and caspase-7, which are common to both the death receptor and mitochondrial apoptotic signaling pathways. The apoptotic caspase cascade mediates many of the hallmarks of apoptosis, such as membrane blebbing and phosphatidylserine exposure. Despite this, caspases are ultimately dispensable for intrinsic apoptotic cell death, as irreversible mitochondrial membrane damage caused by BAK and BAX ensures the cells' demise (Ekert et al., 2004; Marsden et al., 2002).

In viable cells, the activation of BAX and BAK (BAX/BAK) is directly held in check by pro-survival BCL-2 family members, including BCL-XL, BCL-2, BCL-W, A1 (BFL-1), and MCL-1 (Kale et al., 2018). Exposure to cytotoxic stimuli often triggers BAX/BAK activation via the induction of pro-apoptotic BH3-only proteins (e.g., BIM, NOXA, PUMA) that potently antagonize pro-survival BCL-2 proteins. Consequently, a number of anti-cancer BH3-mimetic compounds have been developed that exhibit exquisite specificity for several BCL-2 proteins (e.g., ABT-737 targeting of BCL-2, BCL-XL, BCL-W; Oltersdorf et al., 2005; van Delft et al., 2006) or individual family members (e.g., S63845 targeting of MCL-1 [Kotschy et al., 2016] and ABT-199 targeting of BCL-2 [Souers et al., 2013]). Pre-clinical models and subsequent clinical studies have validated their efficacy against cancer (Roberts et al., 2016), and remarkably, emerging studies show how BCL-XL targeted BH3 mimetics might be repurposed to induce death specifically in pathogen-infected host cells to eliminate microbial infection (Speir et al., 2016).

Apoptotic cell death is classically regarded as immunologically silent. This feature is achieved, in part, by limiting plasma

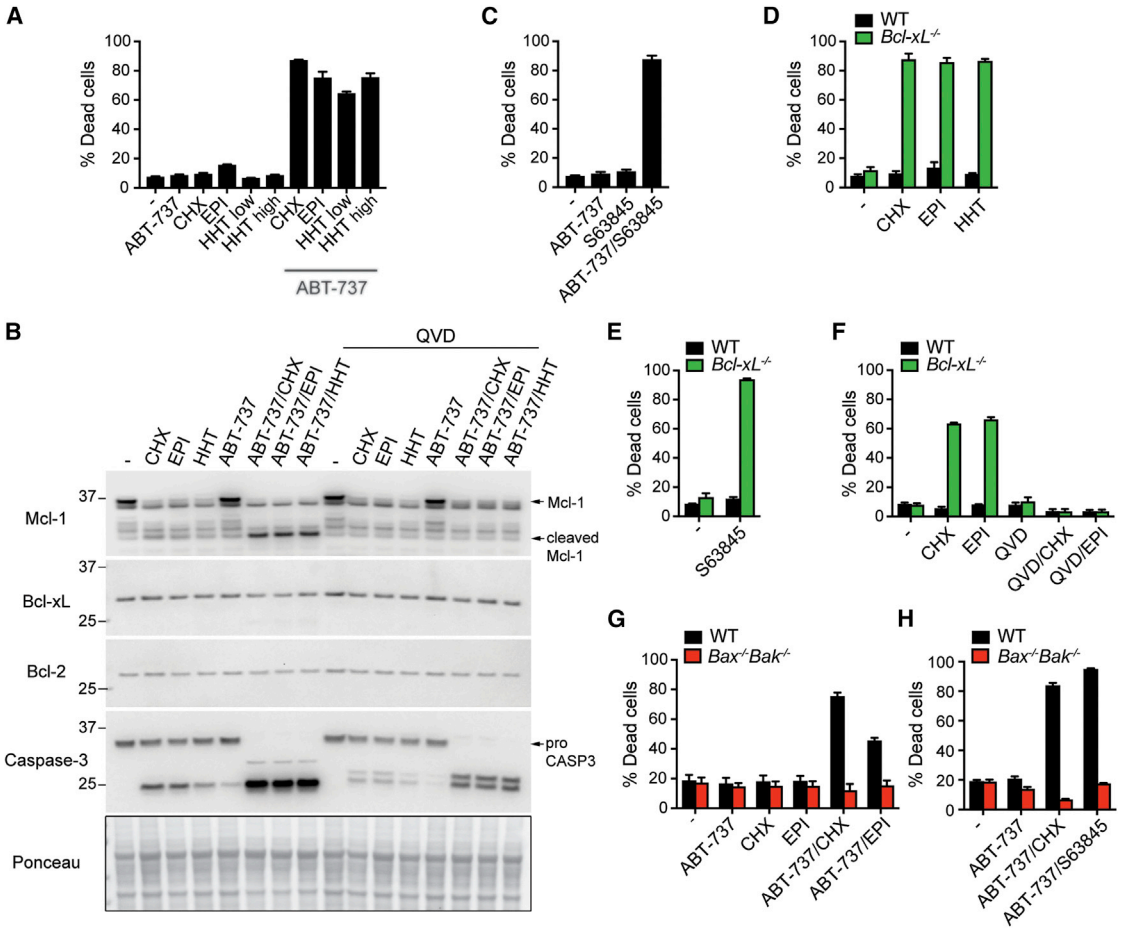

Figure 1. Loss of BCL-XL and MCL-1 in Macrophages Triggers BAX/BAK-Mediated Apoptosis

(A–C) Wild-type (WT) BMDMs were treated with BH3-mimetic ABT-737 (1 μM) alone and/or with protein synthesis inhibitors cycloheximide (CHX; 20 μg/mml), episilvesterol (EPI; 500 nM), homoharringtonine (HHT; low 500 nM and high 1,000 nM), and MCL-1 inhibitor (S63845; 10 μM). In some cases, cells were pre-treated with the pan-caspase inhibitor Q-VD-OPh (QVD; 40 μM).

(A and C) Cell death was assessed by flow cytometric analysis of PI uptake. Data are mean + SEM, n = 3 mice, one of two experiments.

(B) Cell lysates were analyzed by immunoblot after 6 hr. Represents one of two experiments. See also Figure S1.

(D–F) WT and *Bcl-xL*$^{-/-}$ BMDMs were pre-treated with QVD (40 μM) for 30 min, as indicated, and cultured with CHX (20 μg/mL), EPI (500 nM), HHT (1,000 nM), and S63845 (10 μM) for a further 5–6 hr. Cell death was measured by PI uptake and flow cytometry. Data are mean + SEM, n = 3 mice/group, one of at least two experiments.

(G and H) WT and *Bax*$^{-/-}$*Bak*$^{-/-}$ BMDMs were treated with ABT-737 (1 μM) alone and/or CHX (20 μg/mL), EPI (500 nM), and S63845 (10 μM) for 6 hr, and cell viability was assessed by flow cytometric analysis of PI uptake. Data are mean + SEM, n = 3 mice/group, one of three experiments.

membrane breakdown and the lytic release of cellular contents and via the display of "find me" and "eat me" signals to trigger the rapid phagocytic clearance of apoptotic bodies (Fuchs and Steller, 2015). Several studies have also documented how apoptotic caspases inactivate specific inflammatory signaling pathways (Rongvaux et al., 2014; White et al., 2014) and cytokines (Giampazolias et al., 2017; Lüthi et al., 2009). Despite these observations, recent genetic evidence acquired from the study of innate immune cells has shown that death receptor apoptotic signaling, initiated by TNF receptor 1 (TNFR1), Fas, or Toll-like receptors (TLR), can induce potent inflammatory responses both *in vitro* and *in vivo* (Feltham et al., 2017). The inflammatory potential of apoptotic signaling in innate immune cells is perhaps best highlighted by the occurrence of hyperinflammatory disease in humans and mice with mutations or deficiency in negative regulators of TNFR1 and TLR cell death pathways, such as the inhibitor of apoptosis (IAP) family members X-linked IAP (XIAP) and cellular IAP1 (cIAP1) (Lawlor et al., 2017; Vince and Silke, 2016). Of note, we and others have shown that in most of these cases the TLR- or TNFR1-induced death receptor initiator caspase, caspase-8, drives activation of the potent pro-inflammatory cytokine IL-1β in innate immune cells (Chen et al., 2018; Gaidt et al., 2016; Lawlor et al., 2015; Maelfait et al., 2008; Moriwaki et al., 2015; Vince et al., 2012; Wicki et al., 2016; Yabal et al., 2014).

Activated caspase-8 can directly process precursor IL-1β to its mature bioactive 17 kDa form (Bossaller et al., 2012; Maelfait et al., 2008; Vince et al., 2012). In some circumstances,

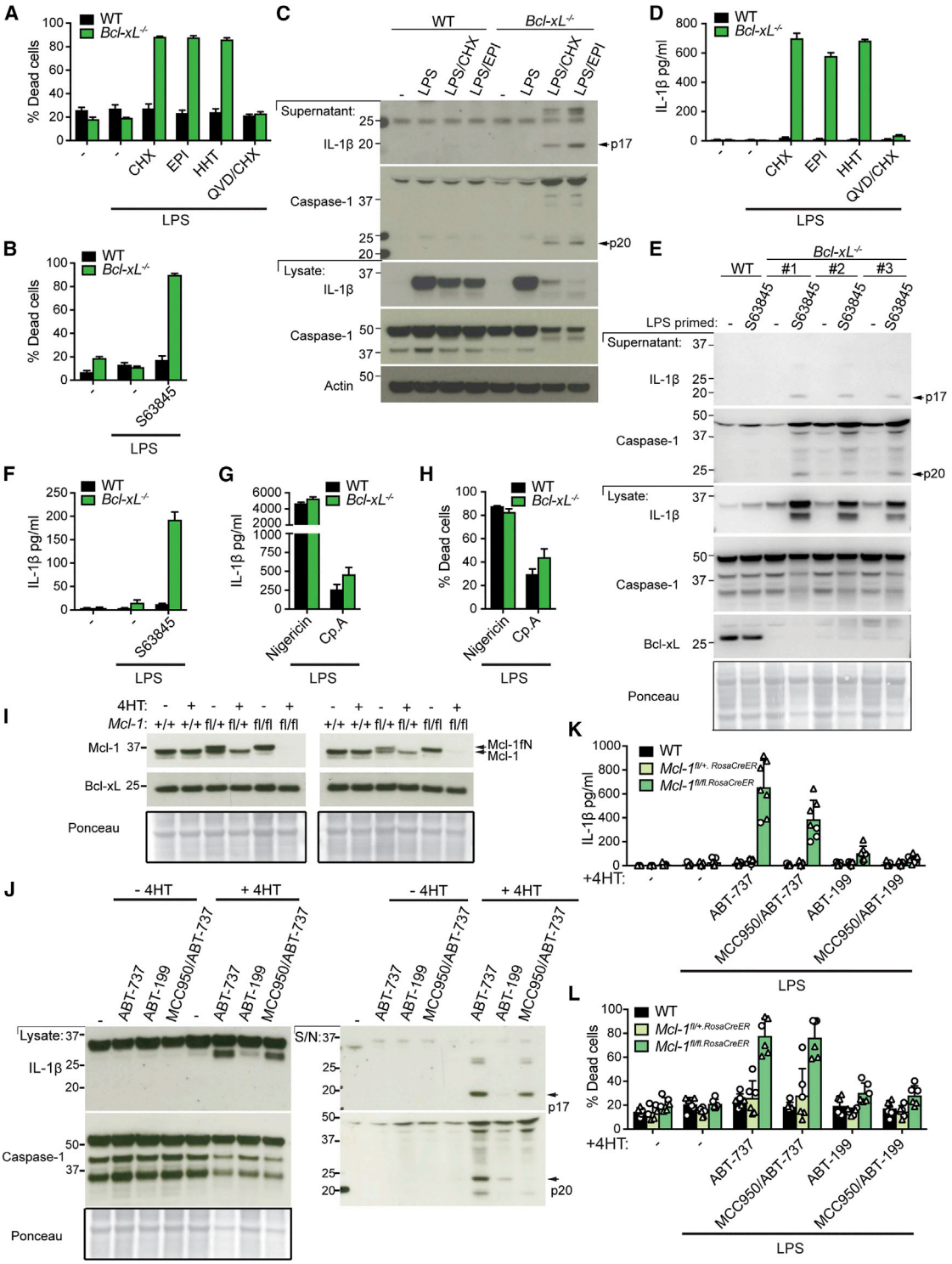

Figure 2. BCL-XL and MCL-1 Targeting Renders Macrophages Sensitive to Caspase-1 and IL-1β Activation

WT and *Bcl-xL*$^{-/-}$ BMDMs were primed for 2–3 hr with LPS (50 ng/mL), pre-treated with QVD (20–40 μM) in the final 30 min of priming, as indicated, and treated with CHX (20 μg/mL), EPI (500 nM), HHT (1,000 nM), S63845 (10 μM), or compound A (Cp. A) (911; 1,000 nM) for 5–6 hr or nigericin (10 μM) for 1 hr.

(A, B, and H) Cell death was measured by PI uptake and flow cytometry.

(C and E) Cell lysates and supernatants were analyzed by immunoblot.

(legend continued on next page)

particularly following IAP loss in murine macrophages (Lawlor et al., 2015, 2017; Vince et al., 2012) or TLR stimulation of human monocytes (Gaidt et al., 2016), caspase-8 can also trigger NOD-like receptor-3 (NLRP3) inflammasome assembly to activate the inflammatory caspase, caspase-1. Caspase-1 subsequently cleaves IL-1β, and with canonical inflammasome triggers it also facilitates IL-1β release via activation of the membrane pore-forming protein, gasdermin D (GSDMD). As such, GSDMD is required for efficient caspase-1-mediated cell lysis, pyroptosis, and, in many cases, the release of bioactive IL-1β (He et al., 2015; Kayagaki et al., 2015; Shi et al., 2015). Whether apoptosis signaling emanating from the essential intrinsic apoptotic effector proteins BAX and BAK can generate pro-inflammatory signals, akin to death receptor signaling in innate immune cells, remains unclear.

RESULTS

Loss of MCL-1 and BCL-XL Triggers BAX/BAK-Mediated Cell Death in Macrophages

Protein synthesis inhibitors, such as cycloheximide (CHX), episilvesterol (EPI), and homoharringtonine (HHT; omacetaxine mepesuccinate), rapidly deplete the short-lived pro-survival BCL-2 family member MCL-1 (Goodall et al., 2016; Lindqvist et al., 2012), which can be a major contributor to their clinical efficacy (e.g., HHT) in killing cancer cells (Chen et al., 2011; Tang et al., 2006). Similar to these compounds, we recently discovered that *Legionella* bacteria inhibit host macrophage protein synthesis to decrease MCL-1 levels (Speir et al., 2016). However, in this scenario, antagonism of BCL-XL is also required to induce rapid cell death of infected macrophages, suggesting that both MCL-1 and BCL-XL are required for macrophage survival.

Consistent with this idea, we found that wild-type (WT) bone marrow-derived macrophages (BMDMs) were not sensitive to cell death following treatment with the BH3 mimetic ABT-737, a potent inhibitor of BCL-XL, BCL-W, and BCL-2 (Figures 1A and S1A). However, BMDMs rapidly succumbed to apoptotic caspase activation and cell death when ABT-737 was combined with CHX, EPI, or HHT (Figures 1A, 1B, S1A, and S1B). Protein synthesis inhibition depleted total cellular MCL-1 upstream of caspase activity (i.e., MCL-1 loss was not blocked upon pan-caspase inhibition with Q-VD-OPh [QVD]; Figures 1B and S1B). Importantly, specific inhibition of MCL-1 using S63845 (Kotschy et al., 2016; Merino et al., 2017) in combination with chemical targeting or genetic deficiency of BCL-XL mirrored results with protein synthesis inhibition, demonstrating that MCL-1 and BCL-XL are critical for macrophage survival (Figures 1C–1F). As expected, pan-caspase inhibition using QVD (Figures 1B and 1F) or genetic deletion of BAX and BAK (Figures 1G and 1H) blocked the rapid cell death induced by functional loss of BCL-XL and MCL-1, confirming that the cell death observed was a result of mitochondrial apoptosis.

Loss of MCL-1 and BCL-XL Triggers BAX/BAK-Mediated Activation of IL-1β

We have documented that inflammasome activation resulting from treatment with soluble (e.g., ATP, nigericin) or particulate (e.g., alum) NLRP3 activators was not altered upon deletion of BAX/BAK or overexpression of BCL-2, demonstrating that mitochondrial apoptosis is dispensable for canonical NLRP3 activity (Allam et al., 2014; Lawlor et al., 2013). We were therefore surprised to observe that MCL-1 depletion following treatment with protein synthesis inhibitors CHX, EPI, or HHT, or the MCL-1 inhibitor S63845, not only induced caspase-dependent cell death (Figures 2A, 2B, and S1C) but also increased the cleavage and release of inflammasome-associated caspase-1 and IL-1β in lipopolysaccharide (LPS)-primed *Bcl-xL*$^{-/-}$ BMDMs compared with WT cells (Figures 2C–2F and S1D). In contrast, TLR-induced TNF secretion was not affected by BCL-XL deficiency (Figure S1E). Likewise, IL-1β release (Figure 2G), cell death (Figure 2H), and TNF secretion (Figure S1F) were all comparable between LPS-primed WT and *Bcl-xL*$^{-/-}$ BMDMs in response to treatment with the canonical NLRP3 activator nigericin, or stimulation with the Smac mimetic compound A (Cp. A; antagonizes IAPs) that triggers alternative caspase-8-driven activation of NLRP3 (Lawlor et al., 2015).

To genetically confirm that MCL-1 loss was requisite for macrophage cell death and IL-1β activation following BCL-XL targeting, we treated *Mcl-1*$^{fl/fl}$/*Rosa-cre*^{ER} BMDMs with 4-hydroxytamoxifen (4HT) to generate MCL-1-deficient macrophages (Glaser et al., 2012; Okamoto et al., 2014). Of note, *Mcl-1*$^{fl/fl}$ animals express a 13-residue extended N terminus MCL-1, termed MCL-1-fN (Okamoto et al., 2014), which can be distinguished from WT MCL-1 by immunoblot (Figure 2I). Importantly, the genetic deletion of MCL-1 mirrored results obtained by chemical MCL-1 targeting, with significant caspase-1 and IL-1β activation and secretion (Figures 2J and 2K), as well as cell death (Figure 2L), induced upon BCL-XL inhibition with ABT-737, but not BCL-2 targeting with ABT-199.

To establish if BAX/BAK activation was obligatory for caspase-1 and IL-1β cleavage and secretion following MCL-1 and BCL-XL loss, we next treated LPS-primed WT and BAX/BAK-deficient macrophages with the protein synthesis inhibitor CHX, or the MCL-1-specific inhibitor S63845, and ABT-737. In accord with previous findings, LPS and CHX treatment alone induced IL-1β proteolysis in a BAX/BAK-independent manner (Figures 3A and 3B), presumably via direct TLR4-induced

(D, F, and G) IL-1β levels were measured in supernatants by ELISA. n = 3 mice/group. Mean + SEM, n = 3 mice/group. Data are representative of one of at least two experiments. See also Figure S1.

(I–L) BMDMs derived from *Mcl-1*$^{flox/flox}$/*RosaCre*^{ER} and indicated *Mcl-1*$^{flox/+}$/*RosaCre*^{ER} or *Mcl-1*$^{+/+}$ control animals were treated with 100 nM of 4-hydroxy tamoxifen (4HT) for 24 hr. Subsequently, 4HT was removed and media replaced. Cells were primed for 2–3 hr with LPS (50 ng/mL), with MCC950 (2 μM) added in the last 30 min of priming, as indicated. BMDMs were subsequently treated with ABT-737 (1 μM) or ABT-199 (1 μM) for 20–24 hr. (I and J) Cells were analyzed by immunoblot for MCL-1 levels (two independent mice shown in I) and (J) caspase-1 and IL-1β activation and secretion detected by immunoblot. Data reflect one of two independent experiments. (K) IL-1β levels were measured in supernatants by ELISA, and (L) cell death was measured by PI uptake and flow cytometry. For (K) and (L), n = 3 independent experiments, with different symbols representing independent experiments containing up to three technical replicates. Mean + SEM.

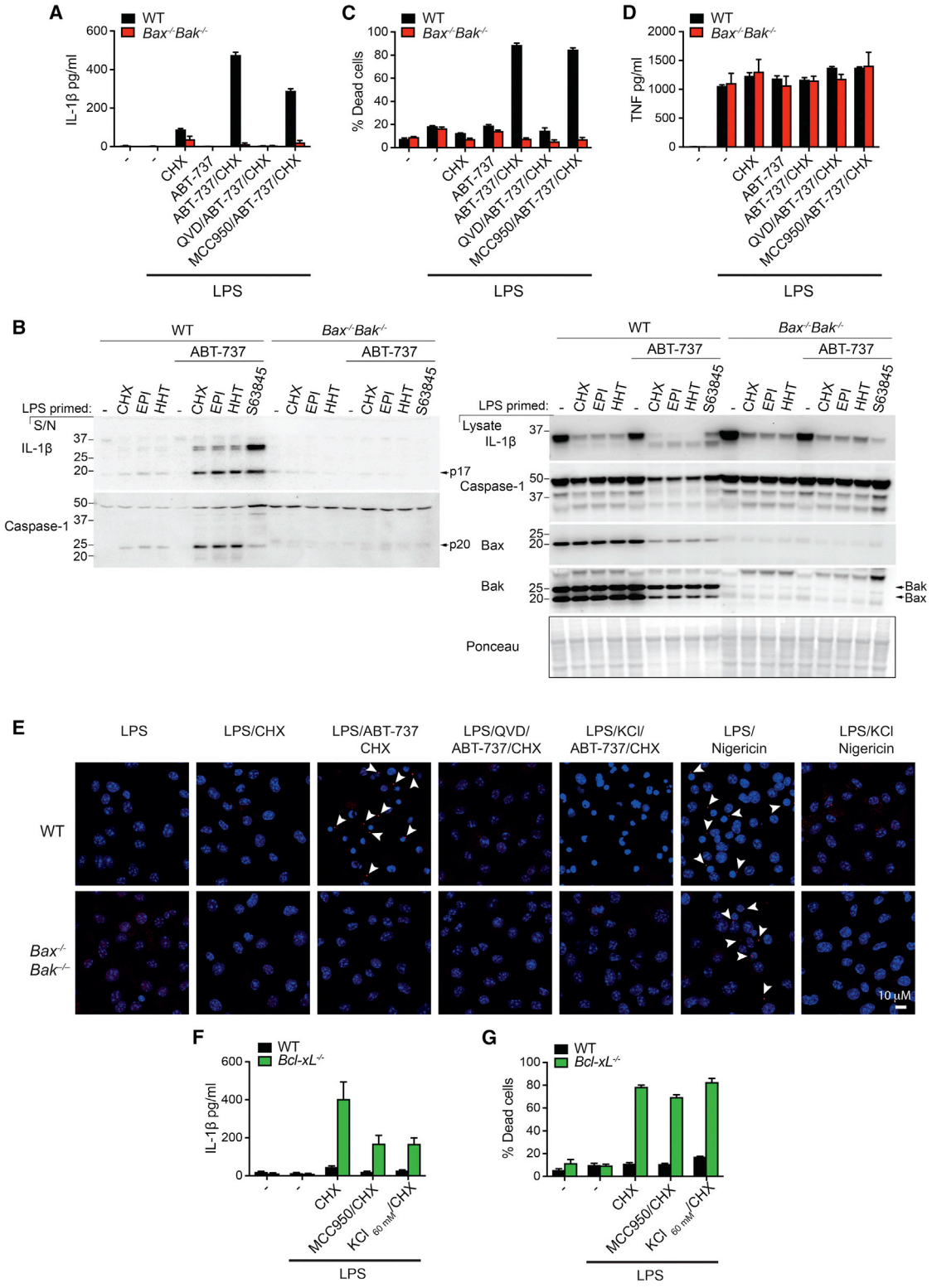

Figure 3. Loss of BCL-XL and MCL-1 Promotes BAX/BAK-Induced NLRP3 and IL-1β Activation

(A–D) WT and $Bax^{-/-}Bak^{-/-}$ BMDMs were primed for 2–3 hr with LPS (50 ng/mL), treated in the last 15–30 min of priming with QVD (20–40 μM) or MCC950 (2 μM), as indicated, and treated with ABT-737 (1 μM) and/or CHX (20 μg/mL) for 6 hr or S63845 for 20 hr. (A) IL-1β and (D) TNF levels were measured in supernatants by

(legend continued on next page)

caspase-8 activity (Allam et al., 2014; Maelfait et al., 2008; Vince et al., 2012). However, chemical targeting of MCL-1 (CHX or S63845) and BCL-XL (ABT-737) markedly increased caspase-1 cleavage and IL-1β secretion, as well as cell death, in WT BMDMs, and this was dependent on BAX and BAK (Figures 3A–3C and S2A–S2D). Importantly, the failure to activate IL-1β and caspase-1 in BAX/BAK-deficient BMDMs did not result from general defects in cytokine production, as reflected by equivalent pro-IL-1β production and TNF secretion in WT and $Bax^{-/-}Bak^{-/-}$ BMDMs (Figures 3B, 3D, S2A, and S2E).

BAX/BAK Signaling Activates the NLRP3 Inflammasome

Mitochondrial damage has been suggested to activate NLRP3 or AIM2 via mtDNA release and direct binding to these inflammasome sensors (Dang et al., 2017; Nakahira et al., 2011; Shimada et al., 2012). We therefore hypothesized that NLRP3 or AIM2 were the most likely inflammasomes triggered by BAX/BAK. Upon activation, these inflammasome sensors recruit the adaptor protein, ASC, which oligomerizes to form a single protein aggregate (so-called ASC speck) to facilitate proximity-mediated activation of caspase-1. Indeed, ABT-737 and CHX treatment of LPS-primed WT, but not $Bax^{-/-}Bak^{-/-}$ BMDMs, resulted in endogenous perinuclear ASC speck formation (Figure 3E). To test the role of NLRP3 in BAX/BAK-dependent IL-1β activation, we first inhibited NLRP3 using the specific chemical inhibitor MCC950 (Coll et al., 2015). NLRP3 inhibition reduced BAX/BAK-mediated IL-1β release and completely prevented caspase-1 processing in WT BMDMs but did not affect cell death (Figures 2J–2L, 3A, 3C, and S2A). In agreement with these data, incubating WT BMDMs with high levels of extracellular potassium to prevent NLRP3 activation via potassium efflux (Muñoz-Planillo et al., 2013; Pétrilli et al., 2007) abrogated BAX/BAK-dependent ASC speck formation but did not prevent apoptosis (i.e., nuclear condensation; Figure 3E). In contrast, the canonical NLRP3 activator nigericin induced potassium efflux-dependent ASC speck formation in both WT and $Bax^{-/-}Bak^{-/-}$ macrophages (Figure 3E). MCC950 or high extracellular potassium treatment also reduced IL-1β and caspase-1 processing and secretion in BCL-XL-deficient BMDMs upon LPS and CHX treatment (Figures 3F and S2G). In contrast, NLRP3 inhibition did not alter cell death and TNF release in BCL-XL-deficient BMDMs, compared with WT cells (Figures 3G and S2F). Collectively, these results suggest that BAX/BAK signaling culminates in IL-1β activation, at least in part, via NLRP3 inflammasome assembly.

We next sought to genetically confirm that NLRP3 is the major activator of caspase-1 downstream of BAX/BAK signaling. Similar to MCC950 treatment, genetic deletion of NLRP3 prevented ABT-737/CHX- and ABT-737/S63845-induced caspase-1 activation and impaired IL-1β secretion (Figures 4A, 4B, S3A, and S3B) but had no effect on cell death or TNF production (Figures 4C, 4D, and S3C). Deficiency in caspase-1 (and caspase-11; due to the 129 strain-associated inactivating caspase-11 mutation; Kayagaki et al., 2011) had comparable effects to NLRP3 loss (Figures 4A–4D and S3A–S3C). On the other hand, deletion of the DNA-sensing AIM2 inflammasome had no impact on BAX/BAK-induced IL-1β and caspase-1 activation (Figures S3D and S3E). Importantly, examination of ASC speck formation in WT and $Nlrp3^{-/-}$ BMDMs confirmed that NLRP3 is required for ASC speck formation upon ABT-737 and CHX treatment, akin to the canonical NLRP3 activator nigericin (Figure 4E). Interestingly, inhibition of caspase activity using QVD blocked ASC speck formation in WT BMDMs following ABT-737 and CHX treatment (Figure 4E), suggesting that BAX/BAK-induced caspase activity acts upstream to trigger NLRP3.

In view of the contribution of caspase-1 in IL-1β secretion during BAX/BAK signaling, we also queried the role of GSDMD. Activation of BAX/BAK using ABT-737 and CHX induced GSDMD cleavage, and this was detected at the same time as caspase-1 processing (Figure S3F). However, GSDMD was not necessary for BAX/BAK-dependent IL-1β release or cell death (Figures 4F, 4G, S3G, and S3H), nor did GSDMD loss affect TNF production (Figures 4H and S3I). This contrasts the important role of GSDMD for canonical, nigericin-induced NLRP3 responses (Figure 4I).

BAX/BAK-Induced Caspase-1 Activation Occurs Coincident with the Degradation of IAP Proteins and the Activation of Caspase-8

The deletion of NLRP3 or caspase-1 only partly reduced BAX/BAK-driven IL-1β cleavage and release (~50%; Figures 4A and 4B) and, at later time points, had little impact on ABT-737/CHX responses (Figure S3A). This partial dependence on NLRP3 for IL-1β activation is reminiscent of the effect of Smac-mimetic Cp. A in LPS-primed macrophages (Figures 4B and 5A) (Lawlor et al., 2015; Vince et al., 2012). Cp. A is a mimetic of the natural IAP antagonist SMAC/DIABLO (Du et al., 2000; Verhagen et al., 2000; Vince et al., 2007), which can be released from damaged mitochondria into the cytosol to antagonize IAPs. Previously, we documented how genetic, chemical, or physiological (i.e., via TNFR2 signaling) loss of the IAPs, particularly cIAP1 and XIAP, induces caspase-8 activity to cleave pro-IL-1β directly and also activate the NLRP3-caspase-1 inflammasome (Lawlor et al., 2015, 2017; Vince et al., 2012; Yabal et al., 2014). We therefore hypothesized that BAX/BAK activation might trigger IAP loss to promote NLRP3 and IL-1β activation. As predicted,

ELISA. Data are mean + SEM, n = 3 mice/group. (C) Cell viability was assessed by measurement of PI uptake by flow cytometric analysis. Data are mean + SEM, n = 3 mice/group. (B) Cell lysates and supernatants were analyzed by immunoblot. Data represent one of three experiments. See also Figure S2.

(E) WT and $Bax^{-/-}Bak^{-/-}$ BMDMs were primed for 2–3 hr with LPS (50 ng/mL), and treated with KCl (60 mM) in the last 30 min of priming, as indicated, prior to addition of ABT-737 (1 μM) and/or CHX (20 μg/mL) for ~3 hr, or nigericin (10 μM) for 30–40 min. ASC speck formation (Alexa 647; red) and nuclei (DAPI; blue) were assessed by confocal microscopy (40× objective). One of three independent experiments, with the exception of KCl treatment, which is analyzed in a further two independent experiments. Scale bar, 10 μm.

(F and G) WT and $Bcl\text{-}xL^{-/-}$ BMDMs were primed for 2–3 hr with LPS (50 ng/mL), treated with MCC950 (2 μM) or KCl (60 mM) in the final 30 min of priming, as indicated, and treated with CHX (20 μg/mL) for a further 5–6 hr. (F) IL-1β levels were measured in supernatants by ELISA, and (G) cell viability was assessed by measurement of PI uptake by flow cytometric analysis. Data are mean + SEM, n = 3 mice/group, one of at least two experiments. See also Figure S2.

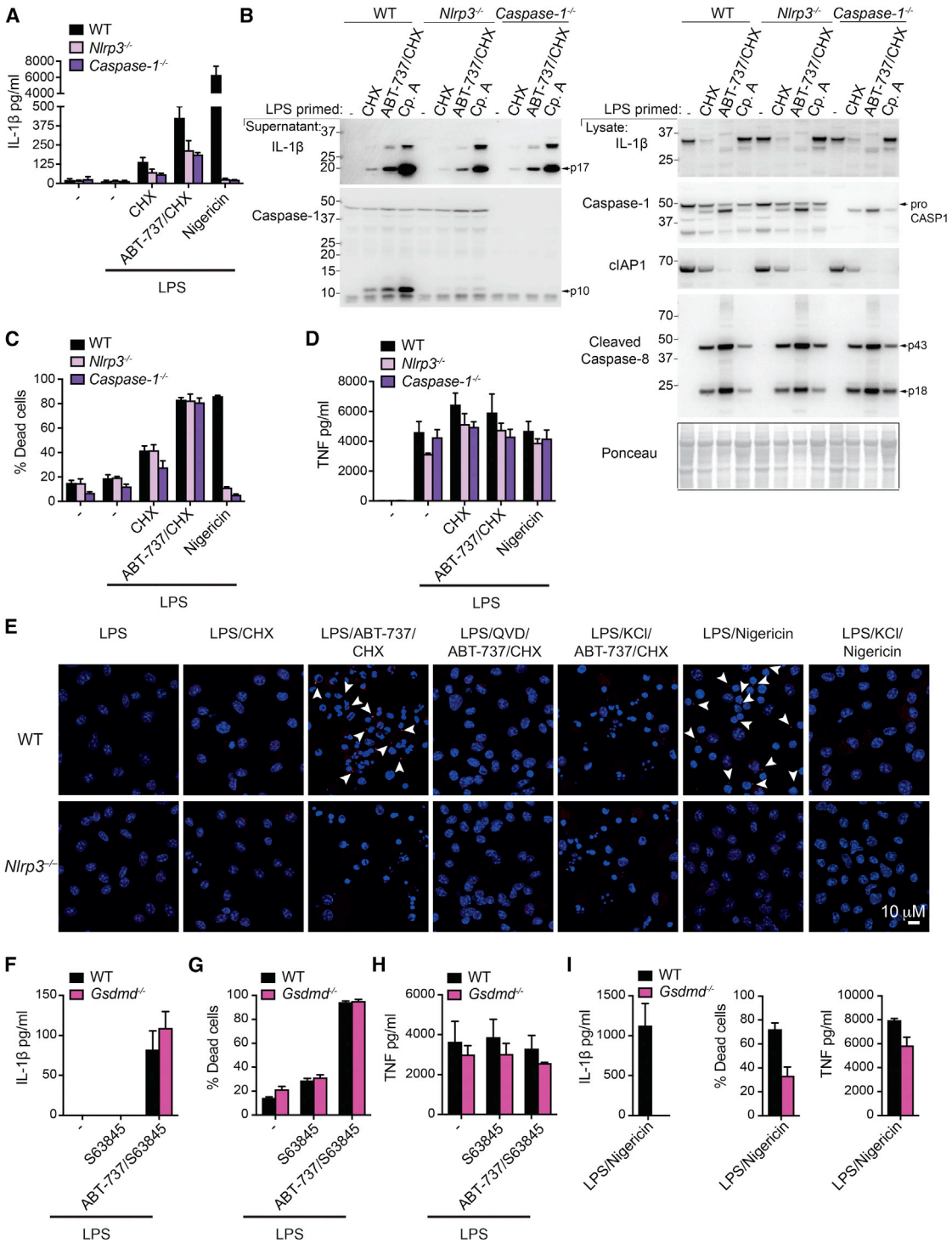

Figure 4. NLRP3 Is Required for ASC Speck Formation and Caspase-1 Activation Downstream of BAX/BAK Signaling

(A–D) WT, *Nlrp3*$^{-/-}$, and *Caspase-1*$^{-/-}$ BMDMs were primed for 3 hr with LPS (50 ng/mL) and treated with ABT-737 (1 μM) and/or CHX (20 μg/mL) for 6 hr or nigericin (10 μM) for 1 hr. (A) IL-1β and (D) TNF levels were measured in supernatants by ELISA. Data are mean + SEM, n = 3 mice/group. (B) Cell lysates and supernatants were analyzed by immunoblot. (C) Cell viability was assessed by measurement of PI uptake by flow cytometric analysis. Data are mean + SEM, n = 3 mice/group. Data represent one of three experiments.

(legend continued on next page)

specific activation of BAX/BAK triggered significant cIAP1 loss in LPS-primed macrophages, and this correlated with the activation of caspase-8, caspase-1, and IL-1β, akin to Cp. A treatment (Figures 4B, 5B, and S1B).

To circumvent the fact that LPS and CHX (or EPI) treatment alone promotes direct TLR-TRIF activation of caspase-8 (Maelfait et al., 2008), we subsequently evaluated BAX/BAK-mediated events in the absence of TLR priming. Importantly, treatment of unprimed BMDMs with ABT-737 and CHX, or the MCL-1 inhibitor S63845, was sufficient to trigger cIAP1 and XIAP loss, caspase-8 activation, and cleavage of caspase-1 (Figures 5C–5E and S4A). Furthermore, these events were dependent on BAX/BAK (Figures 5C and S4A), and caspase-1 processing remained NLRP3 dependent (i.e., abrogated by high extracellular potassium or MCC950; Figures 5D and S3F). These findings demonstrate that BAX/BAK activity causes IAP loss, caspase-8 activation and NLRP3 inflammasome signaling even in the absence of a TLR priming stimulus.

BAX/BAK activation not only induced the rapid degradation of cIAP1 but also triggered XIAP loss and the cleavage of the caspase-8 inhibitor c-FLIP, within ~3 hr (Figures 5E, 5F, and S4A). Pan-caspase inhibition with QVD failed to rescue cIAP1 loss but did limit XIAP depletion and c-FLIP cleavage (Figures 5E, 5F, and S4B). In comparison, pre-treatment with the proteasome inhibitor MG132 alone did not significantly alter cIAP1 or XIAP degradation (Figures 5E, 5F, and S4B). Therefore, BAX/BAK-induced XIAP degradation is dependent on caspase activity, while cIAP1 loss must occur by a combination of events or possibly through another degradation pathway.

BAX/BAK Signaling-Induced Caspase-8 Can Activate IL-1β in the Absence of NLRP3

We queried whether BAX/BAK-induced caspase-8 activity might also cleave IL-1β directly and engage NLRP3, as occurs upon IAP depletion (Lawlor et al., 2015). As caspase-8 deficiency in mice is embryonic lethal because of unrestrained necroptotic cell death (Kaiser et al., 2011; Oberst et al., 2011), we examined BAX/BAK signaling in mice lacking necroptotic receptor interacting protein kinase-3 (RIPK3) and caspase-8 ubiquitously (*Ripk3*$^{-/-}$*Caspase-8*$^{-/-}$) or specifically in myeloid cells (*Caspase-8*^{LysMcre}*Ripk3*$^{-/-}$). In line with our previous findings (Allam et al., 2014), *Ripk3*$^{-/-}$*Caspase-8*$^{-/-}$ BMDMs exhibited reduced precursor IL-1β and TNF levels in response to LPS treatment, which subsequently reduced IL-1β release following nigericin stimulation (Figures 6A, 6B, S4C, and S4D). In comparison, LPS-mediated inflammasome priming, and hence nigericin-induced IL-1β activation, was less affected in *Caspase-8*^{LysMcre}*Ripk3*$^{-/-}$ cells, most likely because of incomplete caspase-8 deletion (Figures 6A, S4C, and S4D). Importantly, caspase-8 deficiency prevented LPS and CHX-induced IL-1β activation (Figures 6A, 6C, and S4E). However, surprisingly, in both LPS-primed *Ripk3*$^{-/-}$*Caspase-8*$^{-/-}$ and *Caspase-8*^{LysMcre}*Ripk3*$^{-/-}$ BMDMs, IL-1β and caspase-1 activation were not prevented upon combined treatment with ABT-737/CHX or ABT-737/S63845 (Figures 6A, 6C, S4E, and S4F), and cell death was comparable with WT responses (Figures S4G and S4H). The appreciable, albeit significantly reduced, levels of IL-1β observed in caspase-8-deficient cells following ABT-737 and CHX stimulation was the result of NLRP3 signaling, as MCC950 limited residual IL-1β activation (Figures S4E and S4F). These results contrasted to those observed following IAP antagonist (Cp. A) treatment, where the caspase-1 and IL-1β secretion (Figures 6A and 6D) and cell death (Figure S4G) observed in LPS-primed WT cells was abolished in both *Ripk3*$^{-/-}$*Caspase-8*$^{-/-}$ and *Caspase-8*^{LysMcre}*Ripk3*$^{-/-}$ BMDMs. Therefore, although caspase-8 activation contributes to direct IL-1β proteolysis upon BAX/BAK activation, BAX/BAK signaling requires a distinct caspase to engage the NLRP3 inflammasome.

BAX/BAK Activation Triggers NLRP3 via Caspase-3 and Caspase-7 Activity

BAX/BAK signaling activates the effector caspases, caspase-3 and caspase-7. Recent reports have shown that active caspase-3 can cleave auto-inhibited gasdermin E (GSDME) to promote pyroptotic-like cell death through the membrane pore-forming activity of the GSDME N-terminal fragment (Rogers et al., 2017; Wang et al., 2017). Considering that BAX/BAK-induced NLRP3 activation was inhibited by preventing cellular potassium ion efflux, we speculated that GSDME could allow potassium ion efflux downstream of BAX and BAK to trigger NLRP3. Upon activation of BAX/BAK in BMDMs, we observed both robust caspase-3 processing and GSDME cleavage to the active N-terminal fragment that was unaffected by MCC950 treatment (Figures 1B and S5A). However, analysis of caspase-3-deficient and GSDME-deficient macrophages revealed that neither of these proteins was essential for NLRP3 activation, IL-1β secretion, and cell death following ABT-737 and CHX treatment (Figures S5B–S5E).

We next considered the possibility that caspase-3 and -7 may act together to trigger NLRP3, particularly as apoptotic caspase activity has been associated with decreased intracellular potassium ion levels (Bortner and Cidlowski, 2007; Park and Kim, 2002). To test this notion, we generated fetal liver-derived macrophages (FLDMs) lacking both caspase-3 and -7. Remarkably, LPS-primed *Caspase-3*$^{-/-}$*Caspase-7*$^{-/-}$ FLDMs treated with ABT-737 and CHX exhibited markedly reduced IL-1β secretion and cell death compared with control cells, despite normal TNF production (Figures 7A–7C and S6) and comparable canonical NLRP3 responses to nigericin (Figures S5F and S6). The lack of BAX/BAK-induced IL-1β release in caspase-3- and -7-deficient macrophages was associated with a loss of ASC speck

(E) WT and *Nlrp3*$^{-/-}$ BMDMs were primed for 2–3 hr with LPS (50 ng/mL), treated with QVD (40 μM) or KCl (60 mM) in the last 30 min of priming, as indicated, prior to addition of ABT-737 (1 μM) and/or CHX (20 μg/mL) for ~3 hr. ASC speck formation (Alexa 647; red) and nuclei (DAPI; blue) were assessed by confocal microscopy (40× objective). One of two independent experiments. Scale bar, 10 μm.

(F–I) WT and *Gsdmd*$^{-/-}$ BMDMs were primed for 3 hr with LPS (50 ng/mL) and treated with ABT-737 (1 μM) and S63845 (845; 10 μM) for 24 hr or nigericin (10 μM) for 1 hr. (F and I) IL-1β and (H and I) TNF levels were measured in supernatants by ELISA. Data are mean + SEM, n = 3 mice/group. (G and I) Cell viability was assessed by measurement of PI uptake by flow cytometric analysis. Data are mean + SEM, n = 3 mice/group. One of three experiments See also Figure S3.

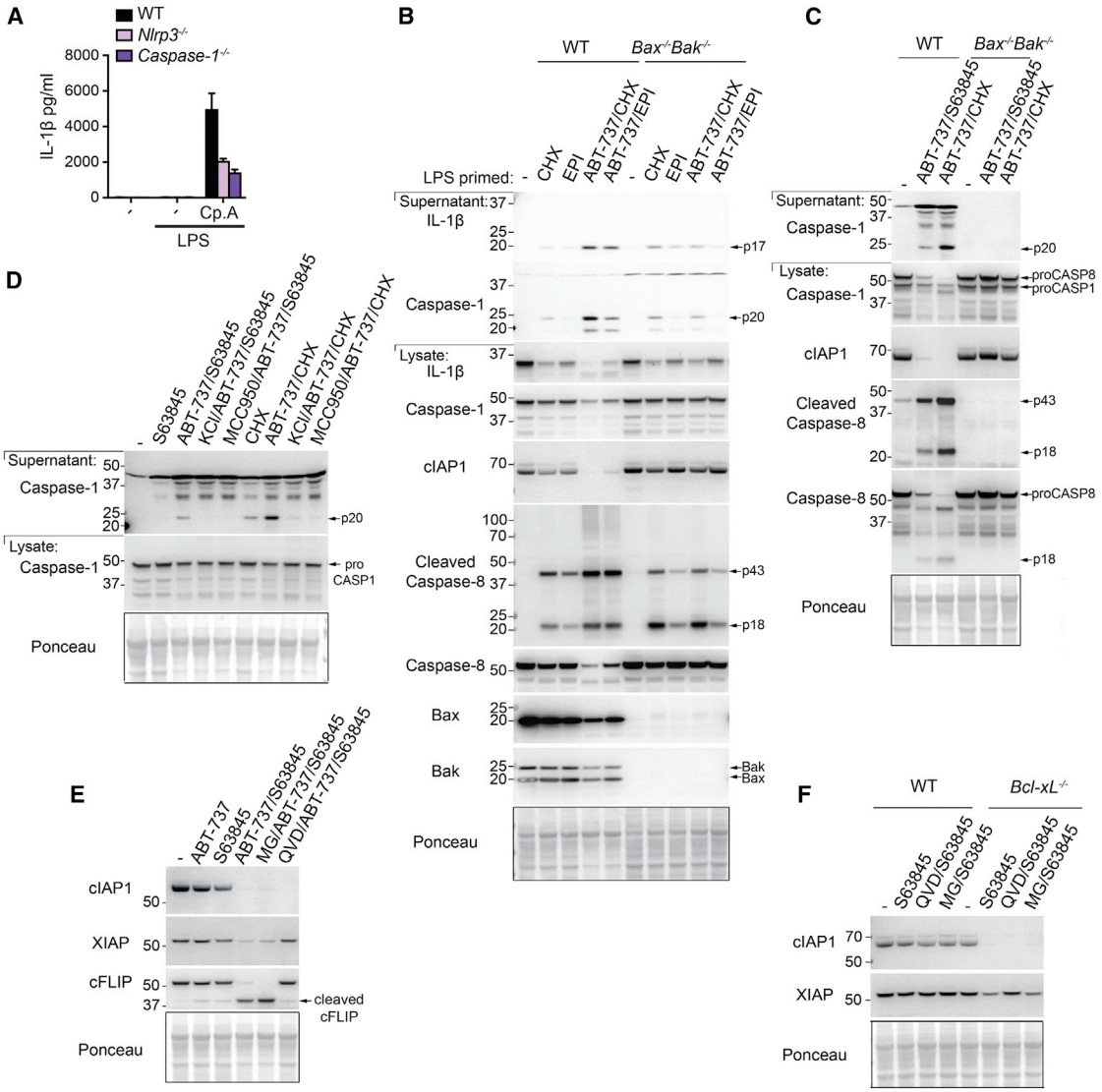

Figure 5. BAX/BAK-Induced NLRP3 and IL-1β Activation Correlates with IAP Loss and Caspase-8 Processing

(A) WT, *Nlrp3*$^{-/-}$, and *Caspase-1*$^{-/-}$ BMDMs were primed for 3 hr with LPS (50 ng/mL) and treated with Smac mimetic Cp. A (1 μM) for a further 6 hr. Supernatants were assayed for IL-1β secretion by ELISA. Data are the mean + SEM, n = 3 mice/group. One of three experiments.

(B) WT and *Bax*$^{-/-}$*Bak*$^{-/-}$ BMDMs were primed with LPS for 3 hr and then treated with ABT-737 (1 μM) and/or CHX (20 μg/mL) or EPI (500 nM) for 6 hr, as indicated. Cell lysates and supernatants were analyzed by immunoblot. Data are one of at least two independent experiments

(C) Unprimed WT and *Bax*$^{-/-}$*Bak*$^{-/-}$ BMDMs were treated with ABT-737 (1 μM) and/or CHX (20 μg/mL) or S63845 (10 μM) for 6 hr, as indicated. Cell lysates and supernatants were analyzed by immunoblot. Data represent one of at least two independent experiments.

(D) Unprimed WT BMDMs were pre-treated with MCC950 (2 μM) or KCl (60 mM) for 30 min, as indicated, and stimulated with ABT-737 (1 μM) and CHX (20 μg/mL) or S63845 (10 μM) for up to 6 hr. Cell lysates and supernatants were analyzed by immunoblot. Data represent one of two independent experiments.

(E and F) Unprimed WT and *Bcl-xL*$^{-/-}$ BMDMs were pre-treated for 30 min with QVD (20–40 μM) or MG132 (MG; 5 μM) prior to stimulation with ABT-737 alone and/or S63845 for a further 2 hr. Cell lysates were analyzed by immunoblot. Data represent one of at least two independent experiments.

See Figure S4A.

formation (Figure 7D) and reduced IL-1β and caspase-1 processing and secretion (Figures 7E and S6). The loss of caspase-3 and -7 in LPS-primed FLDMs did not restore XIAP levels, although it greatly reduced BAX/BAK-induced caspase-8 activation (Figures 7E and S6). Therefore, BAX/BAK signaling activates caspase-3 and -7 to induce both NLRP3 and caspase-8-dependent IL-1β activation.

DISCUSSION

Contrary to the assumption that mitochondrial apoptosis universally shuts down inflammatory responses, we have discovered that the activation of BAX/BAK in macrophages triggers pro-inflammatory IL-1β maturation and release. Our data show that the activation of caspase-3 and -7 downstream of BAX/BAK

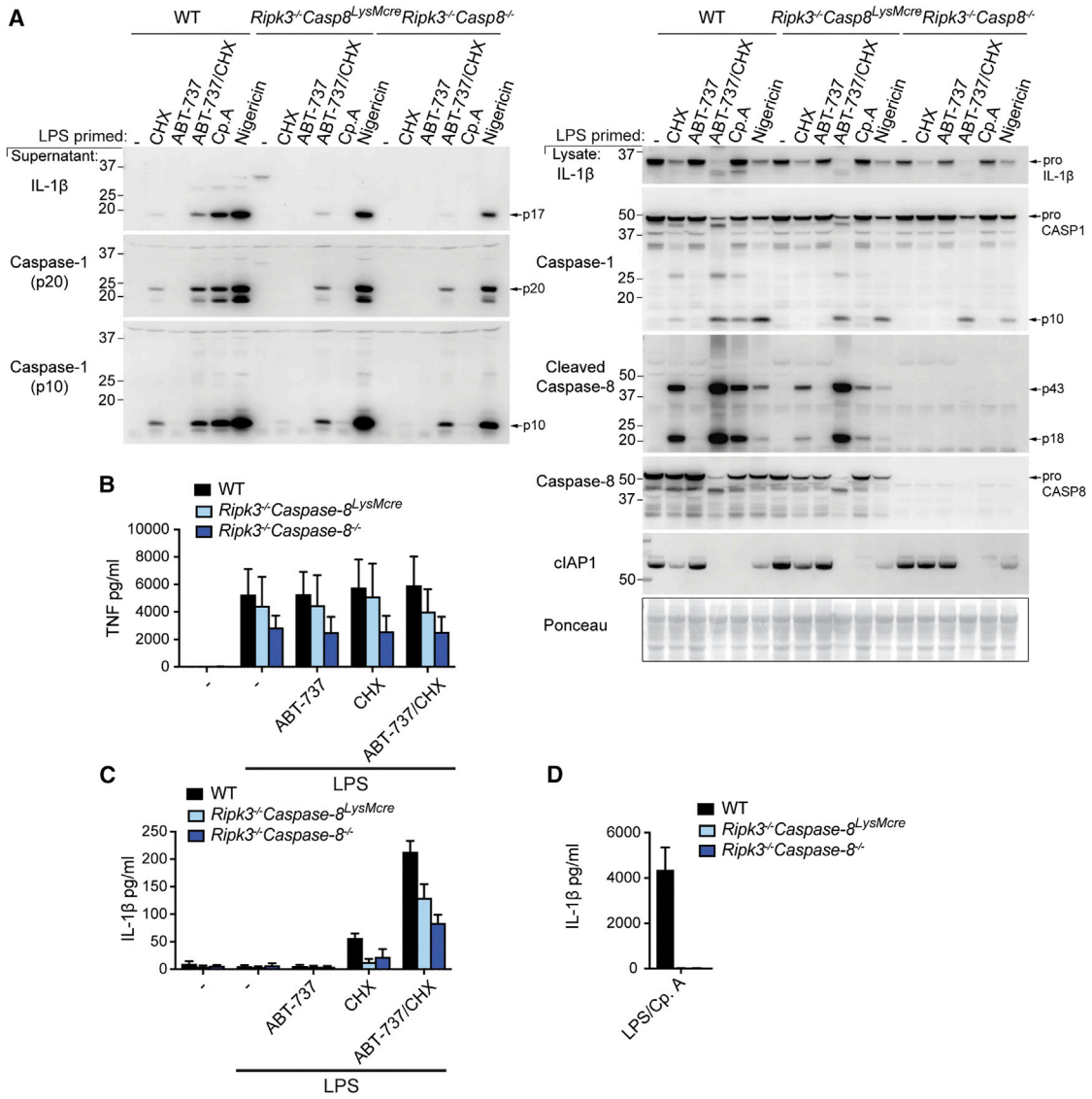

Figure 6. BAX/BAK-Induced Caspase-8 Activity Contributes to IL-1β Cleavage but Is Not Required for NLRP3 and Caspase-1 Activation

(A) WT, *Caspase-8*^{LysMcre}*Ripk3*$^{-/-}$, and *Ripk3*$^{-/-}$*Caspase-8*$^{-/-}$ BMDMs were primed for 3 hr with LPS (50 ng/mL) and treated, as indicated, with ABT-737 (1 μM) and/or CHX (20 μg/mL), or with Cp. A (1 μM) for 6 hr, or with nigericin (10 μM) for 1 hr. Cell lysates and supernatants were analyzed by immunoblot. One of at least two experiments.

(B–D) TNF (B) and IL-1β (C and D) were assayed in supernatants by ELISA. Data are mean + SEM, n = 3 mice/group of one of two experiments.

See related Figure S4.

promotes caspase-8-mediated cleavage and activation of IL-1β and also results in potassium ion efflux to trigger NLRP3 inflammasome formation. These findings may have relevance to anti-cancer chemotherapeutics that can activate BAX and BAK and also trigger NLRP3 (Ghiringhelli et al., 2009; Sauter et al., 2011; Westbom et al., 2015).

The genetic or chemical targeting of BCL-XL and MCL-1 specifically triggered BAX/BAK activation and apoptosis in macrophages. When combined with an inflammasome priming stimulus to induce precursor IL-1β expression and elevate NLRP3 levels, the activation of BAX/BAK sufficed to trigger caspase-1 and IL-1β processing and secretion. Notably, these events correlated with BAX/BAK-mediated degradation of the IAP family members cIAP1 and XIAP, which we have documented to critically suppress caspase-8-driven IL-1β activation following TLR or TNFR1 ligation (Lawlor et al., 2017). Consistent with our model for IL-1β activation upon the chemical or genetic loss of IAPs (Lawlor et al., 2015, 2017), BAX/BAK-induced IL-1β activation also resulted in caspase-8-mediated cleavage and maturation of IL-1β.

How BAX/BAK signaling causes IAP loss remains unclear. The permeabilization of mitochondrial membranes releases a number of mitochondrial proteins, such as SMAC/DIABLO, capable of binding to and inhibiting IAP function (Verhagen et al., 2007).

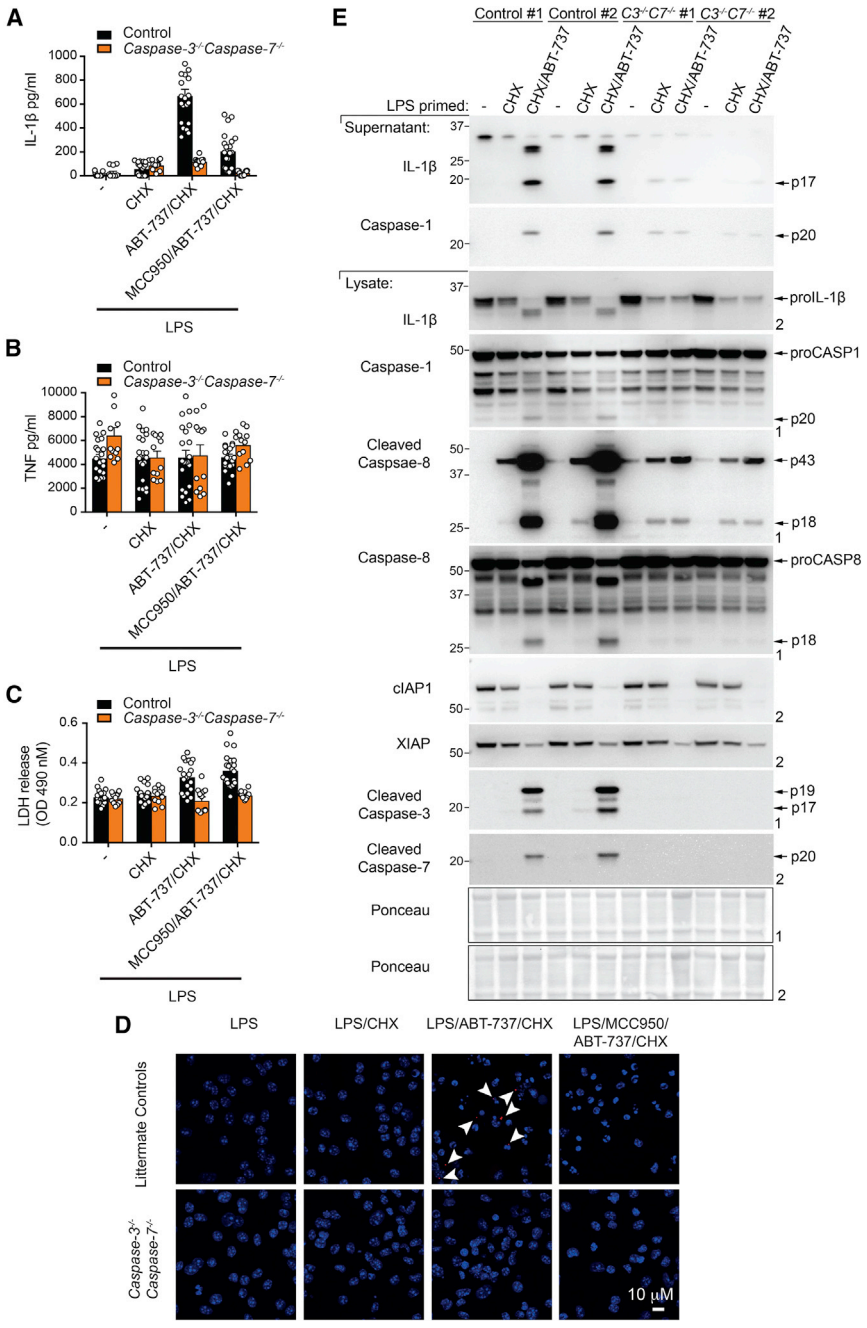

Figure 7. BAX/BAK-Induced Caspase-3 and -7 Activity Promotes Both Caspase-8 and NLRP3 Activation

(A–C) Control (littermates: *Caspase-3*$^{+/-}$*Caspase-7*$^{+/-}$, *Caspase-3*$^{+/-}$*Caspase-7*$^{+/+}$) and *Caspase-3*$^{-/-}$*Caspase-7*$^{-/-}$ FLDMs were primed for 3 hr with LPS (50 ng/mL) and treated in the last 30 min of priming with MCC950 (2 μM), as indicated, and then treated with ABT-737 (1 μM) and/or CHX (20 μg/mL) for 6 hr or nigericin (10 μM) for 1 hr. (A) IL-1β and (B) TNF levels were measured in supernatants by ELISA. (C) Cell viability was assessed by lactate dehydrogenase (LDH) release and are presented as optical density (OD) at 490 nM. Data are mean + SD of triplicate wells, n = 7 control mice and n = 4 *Caspase-3*$^{-/-}$*Caspase-7*$^{-/-}$ mice.

(D) Control and *Caspase-3*$^{-/-}$*Caspase-7*$^{-/-}$ FLDMs were primed for 3 hr with LPS (50 ng/mL), pretreated with MCC950 (2 μM) in the last 30 min, as indicated, prior to addition of ABT-737 (1 μM) and/or CHX (20 μg/mL) for ~3 hr or nigericin (10 μM) for 1 hr. ASC speck formation (Alexa 647; red) and nuclei (DAPI; blue) were assessed by confocal microscopy (40× objective). n = 3 control mice and n = 2 *Caspase-3*$^{-/-}$*Caspase-7*$^{-/-}$ mice. Scale bar, 10 μm.

(E) Control (littermates: *Caspase-3*$^{+/-}$*Caspase-7*$^{+/-}$, *Caspase-3*$^{+/-}$*Caspase-7*$^{+/+}$) and *Caspase-3*$^{-/-}$*Caspase-7*$^{-/-}$ FLDMs (1×10^5/well) were primed for 3 hr with LPS (50 ng/mL) and then treated with ABT-737 (1 μM) and/or CHX (20 μg/mL) for 6 hr. Supernatants and cell lysates were subjected to immunoblot for the specified proteins. n = 2 mice/group. Data represent one of two experiments. See Figures S5 and S6.

Unexpectedly, we observed that BAX/BAK-induced caspase-8 processing and activation required the downstream effector caspases, caspase-3 and -7, which may act to directly process pro-caspase-8 in a feedforward loop to ensure rapid cell death (Ferreira et al., 2012; Tang et al., 2000). It will be interesting to define whether IAP loss is important for optimal BAX/BAK-mediated caspase-3 and -7 activities or only allows efficient processing of pro-caspase-8. Of note, the IAPs are also critical repressors of non-canonical NF-κB (Varfolomeev et al., 2007; Vince et al., 2007), and their degradation following BAX/BAK activation has recently been reported to activate non-canonical NF-κB to initiate inflammatory cytokine production, particularly upon caspase inhibition (Giampazolias et al., 2017). Therefore, BAX/BAK-driven IAP degradation can, in some circumstances, promote both pro-death and pro-inflammatory signaling cascades.

It is possible that redundancy among mitochondrial IAP-binding proteins exists, as a recent report demonstrated that deletion of two mitochondrial IAP-binding proteins, SMAC/DIABLO and OMI, failed to prevent IAP degradation upon intrinsic apoptosis activation (Giampazolias et al., 2017). Consistent with other studies (Deveraux et al., 1999), our data also show that XIAP can be cleaved by caspases downstream of BAX/BAK, which may act to ensure efficient loss of XIAP activity independent of, or in conjunction with, the release of mitochondrial IAP-binding proteins.

Robust BAX/BAK-mediated NLRP3-caspase-1 activation required the effector caspases, caspase-3 and -7, but did not rely on caspase-8 or the pyroptotic effectors GSDMD and GSDME. This is likely to reflect the fact that BAX/BAK

signaling, via the apoptotic effector caspases, caspase-3 and -7, triggers membrane damage or potassium ion channel activation, leading to decreased intracellular potassium ion stores and NLRP3 inflammasome formation. Precisely how potassium ion efflux occurs as a result of caspase-3 and -7 activity remains unclear. Apoptosis-induced activation of potassium ion channels has been suggested to promote cell shrinkage and even death (Kunzelmann, 2016), yet our data demonstrate that potassium ion loss downstream of BAX/BAK is not required for cell death and is not critically dependent on caspase-1/-11 or the caspase-3 lytic effectors GSDMD and GSDME, respectively. Regardless, when taking into consideration the fact that potassium ion efflux is required for pyroptotic caspase-11-induced (Baker et al., 2015; Rühl and Broz, 2015), apoptotic caspase-8-induced (Conos et al., 2017), and necroptotic MLKL-induced (Conos et al., 2017; Gutierrez et al., 2017) NLRP3 inflammasome activation, these results highlight how disruption of membrane integrity resulting from genetically distinct programmed cell death pathways can culminate in pro-inflammatory NLRP3 inflammasome responses.

It has been proposed that mitochondrial apoptotic signaling and consequent oxidized mtDNA release drives NLRP3 inflammasome responses following treatment with canonical NLRP3 activators, such as nigericin and ATP (Shimada et al., 2012). However, even the data of Shimada et al. (2012) showed that oxidized mtDNA acts mainly through the AIM2 inflammasome, and its ability to signal to NLRP3 is, by comparison, limited. Moreover, genetic experiments using mice deficient in BAX/BAK and caspase-9 demonstrated that canonical NLRP3 responses were not affected by the loss of mitochondrial apoptosis (Allam et al., 2014). A recent study also reported that cells depleted of mtDNA can respond normally to the canonical NLRP3 activator ATP to induce IL-1β release (Dang et al., 2017). Nevertheless, despite these controversies, it is clear that cell death-inducing agents, including cancer chemotherapeutics, can activate IL-1β. It will therefore be informative to genetically define which of these clinically useful compounds, in addition to BH3 mimetics, might trigger BAX/BAK-mediated IL-1β to affect anti-cancer immune responses.

STAR★METHODS

Detailed methods are provided in the online version of this paper and include the following:

- KEY RESOURCES TABLE
- CONTACT FOR REAGENT AND RESOURCE SHARING
- EXPERIMENTAL MODEL AND SUBJECT DETAILS
  - Mice
  - Macrophages
- METHOD DETAILS
  - Cell Viability
  - Cytokine analysis
  - ASC specking
  - Immunoblotting
- QUANTIFICATION AND STATISTICAL ANALYSIS

SUPPLEMENTAL INFORMATION

Supplemental Information includes seven figures and can be found with this article online at https://doi.org/10.1016/j.celrep.2018.10.103.

ACKNOWLEDGMENTS

We thank for technical assistance: R. Crawley, L. Wilkins, S. Oliver, and L. Johnson for animal care; S. Monard and staff for flow cytometric sorting; K. Rogers and staff from the Centre for Dynamic Imaging for assistance; TetraLogic Pharmaceuticals for Smac-mimetic compounds; Lorraine O'Reilly for the generous supply of in-house antibodies; Andreas Strasser, Kerstin Brinkmann, and Gemma Kelly (WEHI) and Vishva Dixit (Genentech) for gene targeted mice; and Jennifer M. Chambers for epi-silvesterol synthesis. This work was supported by National Health and Medical Research Project grants (1101405, 1145788, 1099262, 1078763, 1046010, 1051506, and 1127885), fellowships (1052598, 1141466, 1016647, 1090236, 1107149, and 1042629), and program grants (461221 and 1113133), an Australian Federal Government Postgraduate Award, and the DHB Foundation, managed by ANZ Trustees. S.L.M. acknowledges additional funding from the Sylvia and Charles Viertel Foundation, an HHMI-Wellcome International Research Scholarship, and GlaxoSmithKline. This work was also supported by operational infrastructure grants through the Australian Government IRISS (9000220) and the Victorian State Government OIS.

AUTHOR CONTRIBUTIONS

The project was conceived by J.E.V. and K.E.L., the experiments designed by J.E.V., K.E.L., D.D.N., W.G., and the manuscript written by J.E.V. and K.E.L. and edited by G.L., B.T.K., P.B., L.M.L., and D.H.D.G. The experiments were performed by K.E.L., J.E.V., D.D.N., W.G., A.J.V., C.H., D.S., S.V., and L.M.L. Essential mice and reagents were provided by S.M.M., P.B., K.M., M.A.R., J.S., S.L.M., G.L., D.C.S.H., B.T.K., D.H.D.G., and F.S.

DECLARATION OF INTERESTS

J.S. is a former Tetralogic Pharmaceutical Scientific Advisory Board member. J.E.V., D.D.N., A.J.V., C.H., K.M., D.S., S.V., L.M.L., P.B., J.S., S.L.M., G.L., D.S.C.H., B.T.K., and K.E.L. are currently or have been employed at the Walter and Eliza Hall Institute, which received research funding from Servier that holds intellectual rights on S63845 and receive milestone payments in relation to venetoclax (ABT-199) from AbbVie and Genentech. All other authors declare no competing interests.

Received: February 25, 2018
Revised: August 8, 2018
Accepted: October 26, 2018
Published: November 27, 2018

REFERENCES

Adams, T.E., El Sous, M., Hawkins, B.C., Hirner, S., Holloway, G., Khoo, M.L., Owen, D.J., Savage, G.P., Scammells, P.J., and Rizzacasa, M.A. (2009). Total synthesis of the potent anticancer Aglaia metabolites (-)-silvestrol and (-)-episilvestrol and the active analogue (-)-4′-desmethoxyepisilvestrol. J. Am. Chem. Soc. *131*, 1607–1616.

Allam, R., Lawlor, K.E., Yu, E.C., Mildenhall, A.L., Moujalled, D.M., Lewis, R.S., Ke, F., Mason, K.D., White, M.J., Stacey, K.J., et al. (2014). Mitochondrial apoptosis is dispensable for NLRP3 inflammasome activation but non-apoptotic caspase-8 is required for inflammasome priming. EMBO Rep. *15*, 982–990.

Baker, P.J., Boucher, D., Bierschenk, D., Tebartz, C., Whitney, P.G., D'Silva, D.B., Tanzer, M.C., Monteleone, M., Robertson, A.A., Cooper, M.A., et al. (2015). NLRP3 inflammasome activation downstream of cytoplasmic LPS recognition by both caspase-4 and caspase-5. Eur. J. Immunol. *45*, 2918–2926.

Beisner, D.R., Ch'en, I.L., Kolla, R.V., Hoffmann, A., and Hedrick, S.M. (2005). Cutting edge: innate immunity conferred by B cells is regulated by caspase-8. J. Immunol. *175*, 3469–3473.

Bortner, C.D., and Cidlowski, J.A. (2007). Cell shrinkage and monovalent cation fluxes: role in apoptosis. Arch. Biochem. Biophys. *462*, 176–188.

Bossaller, L., Chiang, P.I., Schmidt-Lauber, C., Ganesan, S., Kaiser, W.J., Rathinam, V.A., Mocarski, E.S., Subramanian, D., Green, D.R., Silverman, N., et al. (2012). Cutting edge: FAS (CD95) mediates noncanonical IL-1β and IL-18 maturation via caspase-8 in an RIP3-independent manner. J. Immunol. *189*, 5508–5512.

Chen, R., Guo, L., Chen, Y., Jiang, Y., Wierda, W.G., and Plunkett, W. (2011). Homoharringtonine reduced Mcl-1 expression and induced apoptosis in chronic lymphocytic leukemia. Blood *117*, 156–164.

Chen, K.W., Lawlor, K.E., von Pein, J.B., Boucher, D., Gerlic, M., Croker, B.A., Bezbradica, J.S., Vince, J.E., and Schroder, K. (2018). Cutting edge: blockade of inhibitor of apoptosis proteins sensitizes neutrophils to TNF- but not lipopolysaccharide-mediated cell death and IL-1β secretion. J. Immunol. *200*, 3341–3346.

Coll, R.C., Robertson, A.A., Chae, J.J., Higgins, S.C., Munoz-Planillo, R., Inserra, M.C., Vetter, I., Dungan, L.S., Monks, B.G., Stutz, A., et al. (2015). A small-molecule inhibitor of the NLRP3 inflammasome for the treatment of inflammatory diseases. Nat. Med. *21*, 248–255.

Conos, S.A., Chen, K.W., De Nardo, D., Hara, H., Whitehead, L., Núñez, G., Masters, S.L., Murphy, J.M., Schroder, K., Vaux, D.L., et al. (2017). Active MLKL triggers the NLRP3 inflammasome in a cell-intrinsic manner. Proc. Natl. Acad. Sci. U S A *114*, E961–E969.

Dang, E.V., McDonald, J.G., Russell, D.W., and Cyster, J.G. (2017). Oxysterol restraint of cholesterol synthesis prevents AIM2 inflammasome activation. Cell *171*, 1057–1071.e11.

Deveraux, Q.L., Leo, E., Stennicke, H.R., Welsh, K., Salvesen, G.S., and Reed, J.C. (1999). Cleavage of human inhibitor of apoptosis protein XIAP results in fragments with distinct specificities for caspases. EMBO J. *18*, 5242–5251.

Du, C., Fang, M., Li, Y., Li, L., and Wang, X. (2000). Smac, a mitochondrial protein that promotes cytochrome c-dependent caspase activation by eliminating IAP inhibition. Cell *102*, 33–42.

Ekert, P.G., Read, S.H., Silke, J., Marsden, V.S., Kaufmann, H., Hawkins, C.J., Gerl, R., Kumar, S., and Vaux, D.L. (2004). Apaf-1 and caspase-9 accelerate apoptosis, but do not determine whether factor-deprived or drug-treated cells die. J. Cell Biol. *165*, 835–842.

Feltham, R., Vince, J.E., and Lawlor, K.E. (2017). Caspase-8: not so silently deadly. Clin. Transl. Immunology *6*, e124.

Ferreira, K.S., Kreutz, C., Macnelly, S., Neubert, K., Haber, A., Bogyo, M., Timmer, J., and Borner, C. (2012). Caspase-3 feeds back on caspase-8, Bid and XIAP in type I Fas signaling in primary mouse hepatocytes. Apoptosis *17*, 503–515.

Fuchs, Y., and Steller, H. (2015). Live to die another way: modes of programmed cell death and the signals emanating from dying cells. Nat. Rev. Mol. Cell. Biol. *16*, 329–344.

Gaidt, M.M., Ebert, T.S., Chauhan, D., Schmidt, T., Schmid-Burgk, J.L., Rapino, F., Robertson, A.A., Cooper, M.A., Graf, T., and Hornung, V. (2016). Human monocytes engage an alternative inflammasome pathway. Immunity *44*, 833–846.

Ghiringhelli, F., Apetoh, L., Tesniere, A., Aymeric, L., Ma, Y., Ortiz, C., Vermaelen, K., Panaretakis, T., Mignot, G., Ullrich, E., et al. (2009). Activation of the NLRP3 inflammasome in dendritic cells induces IL-1beta-dependent adaptive immunity against tumors. Nat. Med. *15*, 1170–1178.

Giampazolias, E., Zunino, B., Dhayade, S., Bock, F., Cloix, C., Cao, K., Roca, A., Lopez, J., Ichim, G., Proïcs, E., et al. (2017). Mitochondrial permeabilization engages NF-κB-dependent anti-tumour activity under caspase deficiency. Nat. Cell Biol. *19*, 1116–1129.

Glaser, S.P., Lee, E.F., Trounson, E., Bouillet, P., Wei, A., Fairlie, W.D., Izon, D.J., Zuber, J., Rappaport, A.R., Herold, M.J., et al. (2012). Anti-apoptotic Mcl-1 is essential for the development and sustained growth of acute myeloid leukemia. Genes Dev. *26*, 120–125.

Goodall, K.J., Finch-Edmondson, M.L., van Vuuren, J., Yeoh, G.C., Gentle, I.E., Vince, J.E., Ekert, P.G., Vaux, D.L., and Callus, B.A. (2016). Cycloheximide can induce Bax/Bak dependent myeloid cell death independently of multiple BH3-only proteins. PLoS ONE *11*, e0164003.

Gutierrez, K.D., Davis, M.A., Daniels, B.P., Olsen, T.M., Ralli-Jain, P., Tait, S.W., Gale, M., Jr., and Oberst, A. (2017). MLKL activation triggers NLRP3-mediated processing and release of IL-1β independently of gasdermin-D. J. Immunol. *198*, 2156–2164.

He, W.T., Wan, H., Hu, L., Chen, P., Wang, X., Huang, Z., Yang, Z.H., Zhong, C.Q., and Han, J. (2015). Gasdermin D is an executor of pyroptosis and required for interleukin-1β secretion. Cell Res. *25*, 1285–1298.

Jones, J.W., Kayagaki, N., Broz, P., Henry, T., Newton, K., O'Rourke, K., Chan, S., Dong, J., Qu, Y., Roose-Girma, M., et al. (2010). Absent in melanoma 2 is required for innate immune recognition of Francisella tularensis. Proc. Natl. Acad. Sci. U S A *107*, 9771–9776.

Kaiser, W.J., Upton, J.W., Long, A.B., Livingston-Rosanoff, D., Daley-Bauer, L.P., Hakem, R., Caspary, T., and Mocarski, E.S. (2011). RIP3 mediates the embryonic lethality of caspase-8-deficient mice. Nature *471*, 368–372.

Kale, J., Osterlund, E.J., and Andrews, D.W. (2018). BCL-2 family proteins: changing partners in the dance towards death. Cell Death Differ. *25*, 65–80.

Kayagaki, N., Warming, S., Lamkanfi, M., Vande Walle, L., Louie, S., Dong, J., Newton, K., Qu, Y., Liu, J., Heldens, S., et al. (2011). Non-canonical inflammasome activation targets caspase-11. Nature *479*, 117–121.

Kayagaki, N., Stowe, I.B., Lee, B.L., O'Rourke, K., Anderson, K., Warming, S., Cuellar, T., Haley, B., Roose-Girma, M., Phung, Q.T., et al. (2015). Caspase-11 cleaves gasdermin D for non-canonical inflammasome signalling. Nature *526*, 666–671.

Kotschy, A., Szlavik, Z., Murray, J., Davidson, J., Maragno, A.L., Le Toumelin-Braizat, G., Chanrion, M., Kelly, G.L., Gong, J.N., Moujalled, D.M., et al. (2016). The MCL1 inhibitor S63845 is tolerable and effective in diverse cancer models. Nature *538*, 477–482.

Kuida, K., Lippke, J.A., Ku, G., Harding, M.W., Livingston, D.J., Su, M.S., and Flavell, R.A. (1995). Altered cytokine export and apoptosis in mice deficient in interleukin-1 beta converting enzyme. Science *267*, 2000–2003.

Kuida, K., Zheng, T.S., Na, S., Kuan, C., Yang, D., Karasuyama, H., Rakic, P., and Flavell, R.A. (1996). Decreased apoptosis in the brain and premature lethality in CPP32-deficient mice. Nature *384*, 368–372.

Kunzelmann, K. (2016). Ion channels in regulated cell death. Cell. Mol. Life Sci. *73*, 2387–2403.

Lakhani, S.A., Masud, A., Kuida, K., Porter, G.A., Jr., Booth, C.J., Mehal, W.Z., Inayat, I., and Flavell, R.A. (2006). Caspases 3 and 7: key mediators of mitochondrial events of apoptosis. Science *311*, 847–851.

Lawlor, K.E., van Nieuwenhuijze, A., Parker, K.L., Drake, S.F., Campbell, I.K., Smith, S.D., Vince, J.E., Strasser, A., and Wicks, I.P. (2013). Bcl-2 overexpression ameliorates immune complex-mediated arthritis by altering FcγRIIb expression and monocyte homeostasis. J. Leukoc. Biol. *93*, 585–597.

Lawlor, K.E., Khan, N., Mildenhall, A., Gerlic, M., Croker, B.A., D'Cruz, A.A., Hall, C., Kaur Spall, S., Anderton, H., Masters, S.L., et al. (2015). RIPK3 promotes cell death and NLRP3 inflammasome activation in the absence of MLKL. Nat. Commun. *6*, 6282.

Lawlor, K.E., Feltham, R., Yabal, M., Conos, S.A., Chen, K.W., Ziehe, S., Graß, C., Zhan, Y., Nguyen, T.A., Hall, C., et al. (2017). XIAP loss triggers RIPK3- and caspase-8-driven IL-1β activation and cell death as a consequence of TLR-MyD88-induced cIAP1-TRAF2 degradation. Cell Rep. *20*, 668–682.

Lindqvist, L.M., Vikström, I., Chambers, J.M., McArthur, K., Ann Anderson, M., Henley, K.J., Happo, L., Cluse, L., Johnstone, R.W., Roberts, A.W., et al. (2012). Translation inhibitors induce cell death by multiple mechanisms and Mcl-1 reduction is only a minor contributor. Cell Death Dis. *3*, e409.

Lüthi, A.U., Cullen, S.P., McNeela, E.A., Duriez, P.J., Afonina, I.S., Sheridan, C., Brumatti, G., Taylor, R.C., Kersse, K., Vandenabeele, P., et al. (2009).

Suppression of interleukin-33 bioactivity through proteolysis by apoptotic caspases. Immunity *31*, 84–98.

Maelfait, J., Vercammen, E., Janssens, S., Schotte, P., Haegman, M., Magez, S., and Beyaert, R. (2008). Stimulation of Toll-like receptor 3 and 4 induces interleukin-1beta maturation by caspase-8. J. Exp. Med. *205*, 1967–1973.

Marsden, V.S., O'Connor, L., O'Reilly, L.A., Silke, J., Metcalf, D., Ekert, P.G., Huang, D.C., Cecconi, F., Kuida, K., Tomaselli, K.J., et al. (2002). Apoptosis initiated by Bcl-2-regulated caspase activation independently of the cytochrome c/Apaf-1/caspase-9 apoptosome. Nature *419*, 634–637.

Martinon, F., Pétrilli, V., Mayor, A., Tardivel, A., and Tschopp, J. (2006). Gout-associated uric acid crystals activate the NALP3 inflammasome. Nature *440*, 237–241.

Merino, D., Whittle, J.R., Vaillant, F., Serrano, A., Gong, J.N., Giner, G., Maragno, A.L., Chanrion, M., Schneider, E., Pal, B., et al. (2017). Synergistic action of the MCL-1 inhibitor S63845 with current therapies in preclinical models of triple-negative and HER2-amplified breast cancer. Sci. Transl. Med. *9*, 9.

Moriwaki, K., Bertin, J., Gough, P.J., and Chan, F.K. (2015). A RIPK3-caspase 8 complex mediates atypical pro-IL-1β processing. J. Immunol. *194*, 1938–1944.

Muñoz-Planillo, R., Kuffa, P., Martínez-Colón, G., Smith, B.L., Rajendiran, T.M., and Núñez, G. (2013). K^+ efflux is the common trigger of NLRP3 inflammasome activation by bacterial toxins and particulate matter. Immunity *38*, 1142–1153.

Nakahira, K., Haspel, J.A., Rathinam, V.A., Lee, S.J., Dolinay, T., Lam, H.C., Englert, J.A., Rabinovitch, M., Cernadas, M., Kim, H.P., et al. (2011). Autophagy proteins regulate innate immune responses by inhibiting the release of mitochondrial DNA mediated by the NALP3 inflammasome. Nat. Immunol. *12*, 222–230.

Newton, K., Sun, X., and Dixit, V.M. (2004). Kinase RIP3 is dispensable for normal NF-kappa Bs, signaling by the B-cell and T-cell receptors, tumor necrosis factor receptor 1, and Toll-like receptors 2 and 4. Mol. Cell. Biol. *24*, 1464–1469.

Oberst, A., Dillon, C.P., Weinlich, R., McCormick, L.L., Fitzgerald, P., Pop, C., Hakem, R., Salvesen, G.S., and Green, D.R. (2011). Catalytic activity of the caspase-8-FLIP(L) complex inhibits RIPK3-dependent necrosis. Nature *471*, 363–367.

Okamoto, T., Coultas, L., Metcalf, D., van Delft, M.F., Glaser, S.P., Takiguchi, M., Strasser, A., Bouillet, P., Adams, J.M., and Huang, D.C. (2014). Enhanced stability of Mcl1, a prosurvival Bcl2 relative, blunts stress-induced apoptosis, causes male sterility, and promotes tumorigenesis. Proc. Natl. Acad. Sci. U S A *111*, 261–266.

Oltersdorf, T., Elmore, S.W., Shoemaker, A.R., Armstrong, R.C., Augeri, D.J., Belli, B.A., Bruncko, M., Deckwerth, T.L., Dinges, J., Hajduk, P.J., et al. (2005). An inhibitor of Bcl-2 family proteins induces regression of solid tumours. Nature *435*, 677–681.

Park, I.S., and Kim, J.E. (2002). Potassium efflux during apoptosis. J. Biochem. Mol. Biol. *35*, 41–46.

Pétrilli, V., Papin, S., Dostert, C., Mayor, A., Martinon, F., and Tschopp, J. (2007). Activation of the NALP3 inflammasome is triggered by low intracellular potassium concentration. Cell Death Differ. *14*, 1583–1589.

Rickard, J.A., O'Donnell, J.A., Evans, J.M., Lalaoui, N., Poh, A.R., Rogers, T., Vince, J.E., Lawlor, K.E., Ninnis, R.L., Anderton, H., et al. (2014). RIPK1 regulates RIPK3-MLKL-driven systemic inflammation and emergency hematopoiesis. Cell *157*, 1175–1188.

Roberts, A.W., Davids, M.S., Pagel, J.M., Kahl, B.S., Puvvada, S.D., Gerecitano, J.F., Kipps, T.J., Anderson, M.A., Brown, J.R., Gressick, L., et al. (2016). Targeting BCL2 with venetoclax in relapsed chronic lymphocytic leukemia. N. Engl. J. Med. *374*, 311–322.

Rogers, C., Fernandes-Alnemri, T., Mayes, L., Alnemri, D., Cingolani, G., and Alnemri, E.S. (2017). Cleavage of DFNA5 by caspase-3 during apoptosis mediates progression to secondary necrotic/pyroptotic cell death. Nat. Commun. *8*, 14128.

Rongvaux, A., Jackson, R., Harman, C.C., Li, T., West, A.P., de Zoete, M.R., Wu, Y., Yordy, B., Lakhani, S.A., Kuan, C.Y., et al. (2014). Apoptotic caspases prevent the induction of type I interferons by mitochondrial DNA. Cell *159*, 1563–1577.

Rühl, S., and Broz, P. (2015). Caspase-11 activates a canonical NLRP3 inflammasome by promoting K(+) efflux. Eur. J. Immunol. *45*, 2927–2936.

Sauter, K.A., Wood, L.J., Wong, J., Iordanov, M., and Magun, B.E. (2011). Doxorubicin and daunorubicin induce processing and release of interleukin-1beta through activation of the NLRP3 inflammasome. Cancer Biol. Ther. *11*, 1008–1016.

Schindelin, J., Arganda-Carreras, I., Frise, E., Kaynig, V., Longair, M., Pietzsch, T., Preibisch, S., Rueden, C., Saalfeld, S., Schmid, B., et al. (2012). Fiji: an open-source platform for biological-image analysis. Nat. Methods *9*, 676–682.

Shi, J., Zhao, Y., Wang, K., Shi, X., Wang, Y., Huang, H., Zhuang, Y., Cai, T., Wang, F., and Shao, F. (2015). Cleavage of GSDMD by inflammatory caspases determines pyroptotic cell death. Nature *526*, 660–665.

Shimada, K., Crother, T.R., Karlin, J., Dagvadorj, J., Chiba, N., Chen, S., Ramanujan, V.K., Wolf, A.J., Vergnes, L., Ojcius, D.M., et al. (2012). Oxidized mitochondrial DNA activates the NLRP3 inflammasome during apoptosis. Immunity *36*, 401–414.

Souers, A.J., Leverson, J.D., Boghaert, E.R., Ackler, S.L., Catron, N.D., Chen, J., Dayton, B.D., Ding, H., Enschede, S.H., Fairbrother, W.J., et al. (2013). ABT-199, a potent and selective BCL-2 inhibitor, achieves antitumor activity while sparing platelets. Nat. Med. *19*, 202–208.

Speir, M., Lawlor, K.E., Glaser, S.P., Abraham, G., Chow, S., Vogrin, A., Schulze, K.E., Schuelein, R., O'Reilly, L.A., Mason, K., et al. (2016). Eliminating Legionella by inhibiting BCL-XL to induce macrophage apoptosis. Nat. Microbiol. *1*, 15034.

Strasser, A., and Vaux, D.L. (2018). Viewing BCL2 and cell death control from an evolutionary perspective. Cell Death Differ. *25*, 13–20.

Takeuchi, O., Fisher, J., Suh, H., Harada, H., Malynn, B.A., and Korsmeyer, S.J. (2005). Essential role of BAX,BAK in B cell homeostasis and prevention of autoimmune disease. Proc. Natl. Acad. Sci. U S A *102*, 11272–11277.

Tang, D., Lahti, J.M., and Kidd, V.J. (2000). Caspase-8 activation and bid cleavage contribute to MCF7 cellular execution in a caspase-3-dependent manner during staurosporine-mediated apoptosis. J. Biol. Chem. *275*, 9303–9307.

Tang, R., Faussat, A.M., Majdak, P., Marzac, C., Dubrulle, S., Marjanovic, Z., Legrand, O., and Marie, J.P. (2006). Semisynthetic homoharringtonine induces apoptosis via inhibition of protein synthesis and triggers rapid myeloid cell leukemia-1 down-regulation in myeloid leukemia cells. Mol. Cancer Ther. *5*, 723–731.

van Delft, M.F., Wei, A.H., Mason, K.D., Vandenberg, C.J., Chen, L., Czabotar, P.E., Willis, S.N., Scott, C.L., Day, C.L., Cory, S., et al. (2006). The BH3 mimetic ABT-737 targets selective Bcl-2 proteins and efficiently induces apoptosis via Bak/Bax if Mcl-1 is neutralized. Cancer Cell *10*, 389–399.

Varfolomeev, E., Blankenship, J.W., Wayson, S.M., Fedorova, A.V., Kayagaki, N., Garg, P., Zobel, K., Dynek, J.N., Elliott, L.O., Wallweber, H.J., et al. (2007). IAP antagonists induce autoubiquitination of c-IAPs, NF-kappaB activation, and TNFalpha-dependent apoptosis. Cell *131*, 669–681.

Verhagen, A.M., Ekert, P.G., Pakusch, M., Silke, J., Connolly, L.M., Reid, G.E., Moritz, R.L., Simpson, R.J., and Vaux, D.L. (2000). Identification of DIABLO, a mammalian protein that promotes apoptosis by binding to and antagonizing IAP proteins. Cell *102*, 43–53.

Verhagen, A.M., Kratina, T.K., Hawkins, C.J., Silke, J., Ekert, P.G., and Vaux, D.L. (2007). Identification of mammalian mitochondrial proteins that interact with IAPs via N-terminal IAP binding motifs. Cell Death Differ. *14*, 348–357.

Vince, J.E., and Silke, J. (2016). The intersection of cell death and inflammasome activation. Cell. Mol. Life Sci. *73*, 2349–2367.

Vince, J.E., Wong, W.W., Khan, N., Feltham, R., Chau, D., Ahmed, A.U., Benetatos, C.A., Chunduru, S.K., Condon, S.M., McKinlay, M., et al. (2007). IAP antagonists target cIAP1 to induce TNFalpha-dependent apoptosis. Cell *131*, 682–693.

Vince, J.E., Wong, W.W., Gentle, I., Lawlor, K.E., Allam, R., O'Reilly, L., Mason, K., Gross, O., Ma, S., Guarda, G., et al. (2012). Inhibitor of apoptosis proteins limit RIP3 kinase-dependent interleukin-1 activation. Immunity *36*, 215–227.

Wang, Y., Gao, W., Shi, X., Ding, J., Liu, W., He, H., Wang, K., and Shao, F. (2017). Chemotherapy drugs induce pyroptosis through caspase-3 cleavage of a gasdermin. Nature *547*, 99–103.

Westbom, C., Thompson, J.K., Leggett, A., MacPherson, M., Beuschel, S., Pass, H., Vacek, P., and Shukla, A. (2015). Inflammasome modulation by chemotherapeutics in malignant mesothelioma. PLoS ONE *10*, e0145404.

White, M.J., McArthur, K., Metcalf, D., Lane, R.M., Cambier, J.C., Herold, M.J., van Delft, M.F., Bedoui, S., Lessene, G., Ritchie, M.E., et al. (2014). Apoptotic caspases suppress mtDNA-induced STING-mediated type I IFN production. Cell *159*, 1549–1562.

Wicki, S., Gurzeler, U., Wei-Lynn Wong, W., Jost, P.J., Bachmann, D., and Kaufmann, T. (2016). Loss of XIAP facilitates switch to TNFα-induced necroptosis in mouse neutrophils. Cell Death Dis. *7*, e2422.

Yabal, M., Müller, N., Adler, H., Knies, N., Groß, C.J., Damgaard, R.B., Kanegane, H., Ringelhan, M., Kaufmann, T., Heikenwälder, M., et al. (2014). XIAP restricts TNF- and RIP3-dependent cell death and inflammasome activation. Cell Rep. *7*, 1796–1808.

STAR★METHODS

KEY RESOURCES TABLE

REAGENT or RESOURCE	SOURCE	IDENTIFIER
Antibodies		
Rabbit polyclonal anti-ASC	Santa Cruz Biotechnology	Cat#sc-22514-R; RRID: AB_2174874
Rat monoclonal ant-cIAP1	Alexis Biochemicals	Cat#ALX-803-335; RRID: AB_2227905
Mouse monoclonal anti-XIAP (MBL; M044-3)	MBL International Corporation	Cat#M044-3; RRID: AB_592998
Goat polyclonal ant-IL-1β	R&D Systems	Cat#AF-401-NA; RRID: AB_416684
Rabbit polyclonal anti-caspase-1	Santa Cruz Biotechnology	Cat#sc-514; RRID: AB_2068895
Mouse monoclonal anti-caspase-1	Adipogen	Cat# AG-20B-0042-C100; RRID: AB_2490248
Rat monoclonal anti-caspase-8	In house	N/A
Rabbit polyclonal anti-cleaved caspase-8 Asp387	Cell Signaling Technology	Cat#9429; RRID: AB_2068300
Rabbit polyclonal anti-BAX	Cell Signaling Technology	Cat#2772; RRID: AB_10695870
Rabbit polyclonal anti-BAK	Millipore	Cat#06-536; RRID: AB_310159
Mouse monoclonal anti-NLRP3	Adipogen	Cat#AG-20B-0014_C100; RRID: AB_2490202
Rabbit monoclonal anti-MCL-1	Cell Signaling Technology	Cat#5453; RRID: AB_10694494
Rabbit monoclonal anti-BCL-XL	Cell Signaling Technology	Cat#2764; RRID: AB_2228008
Rabbit polyclonal anti-BCL-2	In house	N/A
Rabbit polyclonal anti-caspase-3	Cell Signaling Technology	Cat#9662; RRID: AB_331439
Rabbit polyclonal anti-caspase-7	Cell Signaling Technology	Cat#9492; RRID: AB_2228313
Rat monoclonal anti-cFLIP	Adipogen	Cat#AG-20B-0005; RRID: AB_2490185
Rabbit monoclonal anti-GSDMD	Abcam	Cat#ab209845; RRID not available
Rabbit monoclonal anti-GSDME	Abcam	Cat#ab215191; RRID: AB_2737000
Goat anti-rabbit (H+L) highly cross adsorbed secondary antibody Alexa Fluor 647	Invitrogen	Cat#A-21245; RRID: AB_2535813
Chemicals, Peptides, and Recombinant Proteins		
LPS	InvivoGen	Cat#tlrl-3pelps
Cycloheximide	SIGMA-Aldrich	Cat#C7698
Episilvesterol	In house	N/A
Homoharringtonine	Enzo Life Sciences	Cat# ALX-350-236-M005
S-63845	Active Biochem	Cat#A-6044
ABT-737	Active Biochem	Cat#A-1002
MG132	SIGMA-Aldrich	Cat#SML1135
QVD	MP Biomedicals	Cat#03OPH109
911 (Cp. A)	TetraLogic Pharmaceuticals	N/A
Nigericin	SIGMA-Aldrich	Cat#N7143
MCC950	In house	Provided by A. Roberson and M. Cooper, University of Queensland, Australia
Critical Commercial Assays		
Mouse IL-1 beta/IL-1F2 DuoSet ELISA	R&D Systems	Cat#DY401
Mouse IL-1beta ELISA kit	DAKEWEI	Cat#DKW12-2012-096
Mouse TNF alpha ELISA Ready-SET-Go! Kit	eBioscience	Cat#5017331
Cyto Tox 96 Non-Radioactive Cytotoxicity assay kit	Promega	Cat#G1780
Cytotoxicity detection kit from Roche	Sigma	Cat#11644793001
Experimental Models: Organisms/Strains		
Mouse: *Bcl-xL*$^{flox/flox}$LysM-Cre	Speir et al., 2016	N/A
Mouse: *Caspase-8*$^{flox/flox}$*Ripk3*$^{-/-}$	Beisner et al., 2005; Newton et al., 2004	N/A

(*Continued on next page*)

Continued

REAGENT or RESOURCE	SOURCE	IDENTIFIER
Mouse: *Caspase-8*$^{-/-}$*Ripk3*$^{-/-}$	Beisner et al., 2005; Newton et al., 2004	N/A
Mouse: *Bax*$^{flox/flox}$*Bak*$^{-/-}$	Takeuchi et al., 2005	N/A
Mouse: *Mcl-1*$^{flox/flox}$ Rosa26-Cre-ERT2 (homozygous Cre)	Glaser et al., 2012	N/A
Mouse: *Ripk3*$^{-/-}$*Caspase-8*$^{-/-}$	Rickard et al., 2014	N/A
Mouse: *Caspase-1*$^{-/-}$	Kuida et al., 1995	N/A
Mouse: *Nlrp3*$^{-/-}$	Martinon et al., 2006	N/A
Mouse: *Gsdmd*$^{-/-}$	Shi et al., 2015; Kayagaki et al., 2015	N/A
Mouse: *Gsdme*$^{-/-}$	Wang et al., 2017	N/A
Mouse: *Aim2*$^{-/-}$	Jones et al., 2010	N/A
Mouse: *Caspase-3*$^{-/-}$	Kuida et al., 1996	N/A
Mouse: *Caspase-7*$^{-/-}$	Lakhani et al., 2006	N/A
Software and Algorithms		
ZEN 2012 version 8.1 software	Zeiss	https://www.zeiss.com/microscopy
FIJI software (Image merging)	Schindelin et al., 2012	https://fiji.sc
Image Lab software.	Bio-Rad	http://www.bio-rad.com
WEASEL version 2.7 software	WEHI	http://www.frankbattye.com.au/Weasel/
Prism 7 (version 7.0d)	GraphPad Software	https://www.graphpad.com/scientific-software/prism/

CONTACT FOR REAGENT AND RESOURCE SHARING

Further information and requests for resources and reagents should be directed to and will be fulfilled by Kate Lawlor (kate.lawlor@hudson.org.au).

EXPERIMENTAL MODEL AND SUBJECT DETAILS

Mice

All mice were housed under standard conditions at the Walter and Eliza Hall Institute of Medical Research (WEHI), Australia, and the National Institute of Biological Sciences (NIBS), China. All procedures were approved by the WEHI Animal Ethics Committee (Australia) or the Institutional Animal Care and Use Committee at NIBS (China). None of the mice used in our experiments had been previously used for other procedures. The animals presented a healthy status and were employed independently of their gender for generating macrophages. *Caspase-3* and *Caspase-7* heterozygous mice (Kuida et al., 1996; Lakhani et al., 2006) were intercrossed to yield littermate control (*Caspase-3*$^{+/-}$, *Caspase-7*$^{+/-}$, *Caspase-3*$^{+/-}$*Caspase-7*$^{+/-}$), *Caspase-3*$^{-/-}$ (*Caspase-3*$^{-/-}$*Caspase-7*$^{+/+}$, *Caspase-3*$^{-/-}$*Caspase-7*$^{+/-}$) and *Caspase-3*$^{-/-}$*Caspase-7*$^{-/-}$ embryos. *Bcl-xL*$^{flox/flox}$ and *Caspase-8*$^{flox/flox}$*Ripk3*$^{-/-}$ (Beisner et al., 2005; Newton et al., 2004) mice were crossed with the LysM-Cre transgenic mice to conditionally delete BCL-XL and caspase-8 (and RIPK3) in myeloid cells; they are referred to as *Bcl-xL*$^{-/-}$ (Speir et al., 2016) or *Caspase-8*^{LysMcre}*Ripk3*$^{-/-}$. *Bax*$^{flox/flox}$*Bak*$^{-/-}$ mice (Takeuchi et al., 2005) were crossed with Vav-Cre transgenic mice (or compound knockouts used) to generate mice lacking BAX/BAK in the hematopoietic system and are referred to as *Bax*$^{-/-}$*Bak*$^{-/-}$ mice. *Mcl-1*$^{flox/flox}$ Rosa26-Cre-ERT2 (homozygous Cre), *Ripk3*$^{-/-}$*Caspase-8*$^{-/-}$, *Caspase-1*$^{-/-}$, *Nlrp3*$^{-/-}$, *Gsdmd*$^{-/-}$, and *Gsdme*$^{-/-}$ and *Aim2*$^{-/-}$ mice have been previously described (Glaser et al., 2012; Jones et al., 2010; Kayagaki et al., 2015; Kuida et al., 1995; Martinon et al., 2006; Rickard et al., 2014; Shi et al., 2015; Wang et al., 2017). C57BL/6 and C57BL/6 Ly5.1 mice were purchased from WEHI Bioservices (Kew, Australia). Female and male mice were at least 6 weeks old at the time of experimentation. To expand numbers of *Bax*$^{-/-}$*Bak*$^{-/-}$ mice available for derivation of macrophages, bone marrow and fetal liver cells (~E13.5) were harvested from *Bax*$^{-/-}$*Bak*$^{-/-}$ and WT CD45.2 donor mice. C57BL/6 Ly5.1 (CD45.1) mice were lethally irradiated (2 × 550R) and injected intravenously with 3-5x10^6 cells and allowed to reconstitute for 8 weeks. Levels of reconstitution were assessed using CD45 markers and flow cytometry.

Macrophages

To generate macrophages, bone marrow cells harvested from femoral and tibial bones (6-14 week-old animals of either gender, or > 12 weeks post bone marrow transplantation), or fetal liver cells obtained from E13.5-14 embryos, were cultured in Dulbecco's modified essential medium (DMEM) containing 10% fetal bovine serum (FBS, Sigma), 50 U/ml penicillin and 50 μg/ml streptomycin (complete media) and supplemented with 20% L929 cell conditioned medium for 6 days (37°C, 10% CO_2). Unless otherwise indicated, macrophages were routinely plated at $4x10^5$ cells/well in 24-well tissue culture plates (BD Falcon) or $2x10^5$ cells/well in 96-well flat bottom tissue culture plates. Alternatively, macrophages were plated at $3x10^5$ or $1x10^5$ cells in 24-well or 96-well non-tissue culture treated plates, respectively, for flow cytometric analysis. Macrophages were primed where indicated with LPS (50-100 ng/ml Ultrapure, InvivoGen), for 2-3 hr prior to stimulation as indicated with Cycloheximide (CHX, 20 μg/ml, SIGMA-Aldrich), Episilvesterol (EPI, 500 nM, synthesized by J. Chambers and M. Rizzacasa) according to Rizzacasa et al., (Adams et al., 2009), Homoharringtonine (HHT, 500-1000 nM, Enzo Life Sciences), MCL-1 inhibitor S63845 (Kotschy et al., 2016)(10 μM, Active Biochem), ABT-737 (1 μM, Active Biochem), MG132 (5 μM, SIGMA-Aldrich), QVD (10-40 μM, QVD, MP Biomedicals), 911 (1 μM, Cp. A, TetraLogic Pharmaceuticals), Nigericin (10 μM, SIGMA-Aldrich), KCl (60 mM, SIGMA-Aldrich), MCC950 (2 μM, CP-456773 sodium salt, PZ0280). In some experiments, due to a lower affinity for mouse MCL-1, S63845 was added two times over a 24 hr period, spaced at least 8 hr apart. At specified times supernatants were harvested for cytokine analysis. Supernatants and cells were prepared in reduced sample buffer for immunoblot analysis, and to evaluate cell viability.

METHOD DETAILS

Cell Viability

To evaluate cell viability, supernatants were harvested. Adherent cells from non-tissue culture treated plates were removed using 5 mM EDTA in phosphate buffered saline (PBS) (~3-5 min incubation, room temperature) and these cells added to the supernatants. Dead cells were stained detected by propidium iodide (1-2 μg/ml, PI) uptake and were measured by flow cytometric analysis on a FACS Calibur instrument and Cell quest software (BD Biosciences). FACs data were analyzed using WEASEL version 2.7 software (in-house). In certain experiments (as defined in the figure legends), cell death was evaluated by measuring the release of lactate dehydrogenase (LDH) into supernatants using a cytotoxicity detection kit (LDH) (Roche and Promega) based on the manufacturer's instructions.

Cytokine analysis

IL-1β (R&D and DAKEWEI, DKW12-2012-096) and TNF (Ebioscience) ELISA kits were routinely used to assay cell supernatants for cytokine levels according to the manufacturer's instructions.

ASC specking

Immunofluorescence of endogenous ASC specks was performed as described (Conos et al., 2017). 8-well μ-slides (Ibidi) were coated with 15 μg/ml poly-L-lysine (SIGMA-Aldrich), before relevant BMDMs/FLDMs were seeded at $2x10^5$ cells per well. Cells were primed with LPS (50 ng/ml) for 2-3 hr, treated with or without QVD (40 μM), MCC950 (2 μM) or KCl (60 mM) and stimulated with ABT-737 (1 μM) and CHX (20 μg/ml) for ~3 hr, or Nigericin for 1 hr. Cells were then fixed with 4% paraformaldehyde for 30 min, before blocking and permeablizing cells [Permeabilization buffer: PBS, 10% (v/v) FCS, 0.5% Triton X-100] for 1 hr at room temperature, prior to staining for perinuclear ASC using rabbit anti-ASC (N-15; 1:500; Santa Cruz Biotechnology) overnight at 4°C. Cells were then stained with a secondary donkey anti-rabbit Alexa647 antibody (A-21245; 1:1000; Invitrogen) for 1 hr at room temperature, before nuclear staining with DAPI (1 μM) for 5-10 min. Between each step cells were washed 2-3 times with permeabilization buffer or PBS. Cells were imaged using a Zeiss LSM 780 confocal microscope; 3 × 3 tile scans with Z stacks were obtained for each experimental condition using a 40x oil objective with Immersol 518 F (Zeiss) and acquired with ZEN 2012 version 8.1 software (Zeiss). Image channels were merged and displayed as maximum projection before conversion to tagged image bitmap file (TIFF) using FIJI software (Schindelin et al., 2012).

Immunoblotting

Cell lysates and supernatants (reduced and denatured) were separated on 4%–12% gradient gels (Invitrogen), proteins transferred onto nitrocellulose membrane (Amersham), and ponceau staining performed to evaluate loading accuracy. Membranes were blocked with 5% skimmed milk in PBS containing 0.1% Tween 20 (PBST) for 0.5-1hr and were then probed overnight with primary antibodies (all diluted 1:1000 unless noted otherwise): Mouse β-actin (Sigma; A-1798), GAPDH (Proteintech, 60004-1-Ig), cIAP1 (1:500 ALX-803-335; Alexis Biochemicals), XIAP (MBL; M044-3), pro and mature IL-1β (R&D Systems; AF-401-NA), pro- and cleaved caspase-1 (Santa Cruz; sc-514)(Adipogen; AG-20B-0042-C100), pro-caspase-8 (in-house), cleaved caspase-8 Asp387 (Cell Signaling; 9429), BAX (Cell Signaling; 2772), BAK (Millipore; 06-536), NLRP3 (Adipogen; AG-20B-0014_C100), MCL-1 (Cell Signaling; 5453), BCL-XL (in-house), BCL-2 (in-house), caspase-3 (Cell Signaling; 9662), caspase-7 (Cell Signaling; 9492), c-FLIP (Adipogen; AG-20B-0005), GSDMD (Abcam; ab209845) and GSDME (Abcam; ab215191). Relevant horseradish peroxidase-conjugated secondary antibodies were applied for at least 1-2 hr. Membranes were washed four to six times in PBS-Tween between antibody

incubations. Antibodies were diluted in PBS-Tween containing 5% skimmed milk. Membranes were developed using ECL (Millipore) on an X-OMAT developer (Kodak) or using the ChemiDoc Touch Imaging System (Bio-Rad) and Image Lab software.

QUANTIFICATION AND STATISTICAL ANALYSIS

Flow cytometry data were analyzed using WEASEL version 2.7 software. Error bars (SEM or SD) were calculated using Prism 7 (version 7.0d) as indicated in the figure legends. The number of times each experiment was repeated, and the number of animals used per experiment, are detailed in the figure legends.